

$J=8.5$ Hz), 6.29 (1H, d, $J=16.1$ Hz), 4.22 (2H, t, $J=5.8$ Hz), 3.95 (2H, t, $J=5.8$ Hz), 3.46 (2H, t, $J=8.2$ Hz), 1.65–1.61 (2H, m), 1.34–1.24 (12H, m), 0.88 (3H, t, $J=7.0$ Hz); Anal. Calcd for $C_{25}H_{34}N_2O_3$: C, 73.14; H, 8.35; N, 6.82. Found: C, 73.23; H, 8.46; N, 6.89.

3-{4-Methoxy-3-[2-(nonylpyridin-2-ylamino)ethoxy]phenyl}acrylic Acid (16) Compound 16 was prepared from 21h using the procedure described for 15 in 7.4% yield: colorless oil; $^1\text{H-NMR}$ (CDCl_3 , 500 MHz, δ : ppm) 8.22 (1H, dd, $J=4.9, 1.8$ Hz), 7.69 (1H, d, $J=15.8$ Hz), 7.44 (1H, ddd, $J=8.8, 7.0, 1.8$ Hz), 7.31 (1H, d, $J=1.5$ Hz), 7.09 (1H, dd, $J=8.2, 1.8$ Hz), 6.86 (1H, d, $J=8.2$ Hz), 6.56 (1H, dd, $J=7.0, 5.2$ Hz), 6.51 (1H, d, $J=8.5$ Hz), 6.31 (1H, d, $J=15.8$ Hz), 4.31 (2H, t, $J=6.4$ Hz), 3.99 (2H, t, $J=6.1$ Hz), 3.90 (3H, s), 3.45 (2H, t, $J=7.6$ Hz), 1.65–1.61 (2H, m), 1.32–1.22 (12H, m), 0.88 (3H, t, $J=7.0$ Hz); HR-MS Calcd for $C_{26}H_{36}N_2O_4$ 440.2675, Found 440.2716.

Binding Assay The assay for PPAR binding activity was performed using a CoA-BAP System kit (NuLigand series, Microsystems). Briefly, glutathione-S-transferase-human nuclear receptor ligand binding domain (GST-hNR LBD) fusion proteins were incubated in a glutathione-fixed micro-well plate at 4°C overnight. After excessive proteins were removed, human transcriptional intermediary factor 2 (hTIF2)-bacterial alkaline phosphatase (BAP) fusion proteins were added to the well with test chemicals. After 1 h incubation at 4°C, excessive proteins were removed carefully. The enzyme reaction was allowed to start with the addition of *p*-nitrophenylphosphoric acid (NPP) as a substrate, and incubated at 30°C. After 3 h, the reaction was stopped by the addition of 0.5N aqueous NaOH. The product was measured by reading absorbance at 405 nm with a 1420 ARVO™ multilabel counter (ParkinElmer, Boston, MA, U.S.A.). AP activity was determined by subtracting background absorption from the reading at 405 nm.

Cell-Based Transactivation Assay³⁰ Human embryonic kidney (HEK) 293 cells were cultured in DMEM containing 5% fetal bovine serum at 37°C in a humidified atmosphere of 5% CO₂ in air. Transfections of PPAR and reporter gene constructs were performed by calcium phosphate coprecipitation. Eight hours after transfection, ligands were added. Cells were harvested 12–16 h after treatment, and luciferase and β -galactosidase activities were assayed using a 1420 ARVO™ MX multilabel counter (ParkinElmer, Boston, MA, U.S.A.). DNA cotransfection experiments included 58 ng of reporter plasmid, 12 ng of CMX- β -galactosidase, and 18 ng of each receptor expression plasmid per well in a 96-well plate. Luciferase data were normalized to an internal β -galactosidase control and reported values are the means of triplicate assays.

Preadipocyte Differentiation Test Human preadipocytes from hypodermic tissues, a preadipocyte growth medium and a preadipocyte differentiation medium were purchased from TOYOBO Co., Ltd (Osaka, Japan). Human preadipocytes were cultured for 8 d in preadipocyte growth medium in a humidified incubator at 37°C and 5% CO₂. The medium was renewed every other day. When the preadipocytes reached confluence, the cells were treated with preadipocyte differentiation medium containing compounds 3, 4, or rosiglitazone. The cells were cultured for a further 7 d with the differentiation medium renewed every 3 d. The accumulation of triglycerides was evaluated by measuring the absorbance at 570 nm with a 1420 ARVO™ multilabel counter (ParkinElmer, Boston, MA, U.S.A.) after staining with Lipidos Liquid® (TOYOBO Co., Ltd, Osaka, Japan).

References and Notes

- Nuclear Receptors Nomenclature Committee. *Cell*, **97**, 161–163 (1999).
- Willson T. M., Brown P. J., Sternbach D. D., Henke B. R., *J. Med. Chem.*, **43**, 527–550 (2000).
- Kersten S., Desvergne B., Wahli W., *Nature* (London), **405**, 421–424 (2000).
- Cantello B. C. C., Cawthorne M. A., Cottam G. P., Duff P. T., Haigh D., Hindley R. M., Lister C. A., Smith S. A., Thurlby P. L., *J. Med. Chem.*, **37**, 3977–3985 (1994).
- Momose Y., Meguro K., Ikeda H., Hatanaka C., Oi S., Sohda T., *Chem. Pharm. Bull.*, **39**, 1440–1445 (1991).
- Hauner H., *Diabetes Metab. Res. Rev.*, **18**, S10–S15 (2002).
- Francis G. A., Annicotte J. S., Auwerx J., *Curr. Opin. Pharmacol.*, **3**, 186–191 (2003).
- Lohray B. B., Lohray V. B., Bajji A. C., Kalchar S., Poondra R. R., Padakanti S., Chakrabarti R., Vikramadithyan R. K., Misra P., Juluri S., Mamidi N. V., Rajagopalan R., *J. Med. Chem.*, **44**, 2675–2678 (2001).
- Duran-Sandoval D., Thomas A. C., Bailleul B., Fruchart J. C., Staels B., *Med. Sci.*, **19**, 819–825 (2003).
- Forman B. M., Tontonoz P., Chen J., Brun R. P., Spiegelman B. M., Evans R. M., *Cell*, **83**, 803–812 (1995).
- Kliwer S. A., Lenhard J. M., Willson T. M., Patel I., Morris D. C., Lehmann J. M., *Cell*, **83**, 813–819 (1995).
- Usui S., Suzuki T., Hattori Y., Etoh K., Fujieda H., Nishizuka M., Imagawa M., Nakagawa H., Kohda K., Miyata N., *Bioorg. Med. Chem. Lett.*, **15**, 1547–1551 (2005).
- Buckle D. R., Cantello B. C. C., Cawthorne M. A., Coyle P. J., Dean D. K., Faller A., Haigh D., Hindley R. M., Jecfott L. J., Lister C. A., Pinto I. L., Rami H. K., Smith D. G., Smith S. A., *Bioorg. Med. Chem. Lett.*, **6**, 2121–2126 (1996).
- Buckle D. R., Cantello B. C. C., Cawthorne M. A., Coyle P. J., Dean D. K., Faller A., Haigh D., Hindley R. M., Jecfott L. J., Lister C. A., Pinto I. L., Rami H. K., Smith D. G., Smith S. A., *Bioorg. Med. Chem. Lett.*, **6**, 2127–2130 (1996).
- Hulin B., Newton L. S., Lewis D. M., Genereux P. E., Gibbs E. M., Clark D. A., *J. Med. Chem.*, **39**, 3897–3907 (1996).
- Saurberg P., Pettersson I., Jeppesen L., Bury P. S., Mogensen J. P., Wassermann K., Brand C. L., Sturis J., Woldike H. F., Fleckner J., Andersen A. S., Mortensen S. B., Svensson L. A., Rasmussen H. B., Lehmann S. V., Polivka Z., Sindelar K., Panajotova V., Ynddal L., Wulff E. M., *J. Med. Chem.*, **45**, 789–804 (2002).
- Cronet P., Petersen J. F., Folmer R., Blomberg N., Sjoblom K., Karlsson U., Lindstedt E. L., Bamberg K., *Structure*, **9**, 699–706 (2001).
- Nomura M., Tanase T., Ide T., Tsunoda M., Suzuki M., Uchiki H., Murakami K., Miyachi H., *J. Med. Chem.*, **46**, 3581–3599 (2003).
- Weigand S., Bischoff H., Dittrich-Wengenroth E., Heckroth H., Lang D., Vaupel A., Woltering M., *Bioorg. Med. Chem. Lett.*, **15**, 4619–4623 (2005).
- Kasuga J., Makishima M., Hashimoto Y., Miyachi H., *Bioorg. Med. Chem. Lett.*, **16**, 554–558 (2006).
- Wagaw S., Buchwald S. L., *J. Org. Chem.*, **61**, 7240–7241 (1996).
- Maryanoff B. E., Reitz A. B., *Chem. Rev.*, **89**, 863–927 (1989).
- Grieco P. A., Handy S. T., *Tetrahedron Lett.*, **38**, 2645–2648 (1997).
- Kanayama T., Mamiya S., Nishihara T., Nishikawa J., *J. Biochem. (Tokyo)*, **133**, 791–797 (2003).
- Brown P. J., Stuart L. W., Hurley K. P., Lewis M. C., Winegar D. A., Wilson J. G., Wilkison W. O., Ittoop O. R., Willson T. M., *Bioorg. Med. Chem. Lett.*, **11**, 1225–1227 (2001).
- Sznajdman M. L., Haffner C. D., Maloney P. R., Fivush A., Chao E., Goreham D., Sierra M. L., LeGrumelec C., Xu H. E., Montana V. G., Lambert M. H., Willson T. M., Oliver W. R., Jr., Sternbach D. D., *Bioorg. Med. Chem. Lett.*, **13**, 1517–1521 (2003).
- Usui S., Fujieda H., Suzuki T., Yoshida N., Nakagawa H., Miyata N., *Bioorg. Med. Chem. Lett.*, **16**, 3249–3254 (2006).
- Fukuen S., Iwaki M., Yasui A., Makishima M., Matsuda M., Shimomura I., *J. Biol. Chem.*, **280**, 23653–23659 (2005).
- Henke B. R., *J. Med. Chem.*, **47**, 4118–4127 (2004).
- Lagace D. C., Nachtigal M. W., *J. Biol. Chem.*, **279**, 18851–18860 (2004).
- Relative transactivation activity at 10 μM : compound 4, 163% of WY14643 for α -activity, and 88% of rosiglitazone for γ -activity, compound 8, 275% of WY14643 for α -activity.

Design, synthesis, and biological activity of folate receptor-targeted prodrugs of thiolate histone deacetylase inhibitors

Takayoshi Suzuki,^{a,*} Shinya Hisakawa,^a Yukihiro Itoh,^a Nobuaki Suzuki,^a
Katsumasa Takahashi,^a Masatoshi Kawahata,^b Kentaro Yamaguchi,^b
Hidehiko Nakagawa^a and Naoki Miyata^{a,*}

^aGraduate School of Pharmaceutical Sciences, Nagoya City University, 3-1 Tanabe-dori, Mizuho-ku, Nagoya, Aichi 467-8603, Japan

^bEvaluation Group, Drug Research Department, R&D Division, Pharmaceuticals Group, Nippon Kayaku Co., Ltd, 31-12, Shimo 3-chome, Kita-ku, Tokyo 115-8588, Japan

Received 22 April 2007; revised 10 May 2007; accepted 11 May 2007

Available online 17 May 2007

Abstract—Aiming to develop selective anticancer drugs, we designed and synthesized three disulfides bearing a folic acid moiety as candidate folate receptor (FR)-targeted prodrugs of thiolate histone deacetylase inhibitors. Among them, compound **1** displayed growth-inhibitory activity toward folate receptor-positive MCF-7 breast cancer cells. The activity of **1** was significantly reduced by free folic acid, suggesting that cellular uptake of **1** is mediated by FR.

© 2007 Elsevier Ltd. All rights reserved.

Histone deacetylases (HDACs) have recently emerged as a new target for the development of anticancer drugs, and some small-molecular HDAC inhibitors, including suberoylanilide hydroxamic acid (SAHA) (also known as vorinostat) and MS-275, have been developed as anticancer drugs (Fig. 1).^{1–6} Inhibition of HDACs causes histone hyperacetylation which leads to the disruption of the chromatin structure and the transcriptional activation of genes associated with cancer. Indeed, HDAC inhibitors have shown anticancer activity *in vitro*, in animal models and in patients with solid tumors and hematological malignancies.⁷ Nevertheless, they have been reported to cause adverse events, such as nausea, vomiting, anorexia, anemia, thrombocytopenia, and fatigue, in the course of clinical trials.^{7–9} Therefore, it is necessary to find HDAC inhibitors that show selective anticancer activity.

We have focused on folate receptor (FR)-targeted prodrugs for selectively targeting cancer cells. The vitamin folic acid and its analogues display extremely high affinity for the folate receptor on the cell surface, and are

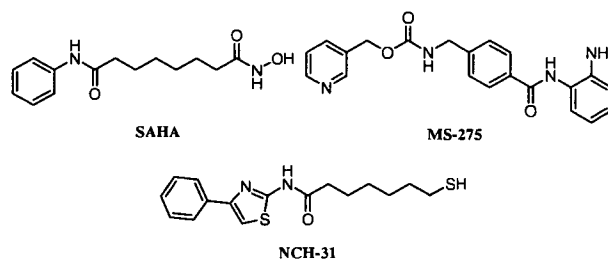


Figure 1. Structures of SAHA, MS-275, and the thiolate HDAC inhibitor NCH-31.

internalized via receptor-mediated endocytosis.¹⁰ Since the FR is overexpressed on certain malignant cell types and is undetectable or present only at low levels in most normal tissues,^{11–13} targeting of the FR has been proposed as a potential mechanism for delivery of drugs to treat cancer.¹⁴ In addition, small molecules including folate-drug conjugates may avoid the limitations associated with antibody-mediated targeting.^{15,16} Here, we report on the design, synthesis, and biological activity of FR-targeted prodrugs of HDAC inhibitors.

We previously reported that thiol-based analogues, including NCH-31 (Fig. 1), are potent HDAC inhibitors.^{17–19} Thiols are thought to inhibit HDACs by coordinating the zinc ion, which is required for deacetylation

Keywords: Histone deacetylase inhibitor; Selective anticancer activity; Folate conjugate; Prodrug.

* Corresponding authors. Tel./fax: +81 52 836 3407; e-mail addresses: suzuki@phar.nagoya-cu.ac.jp; miyata-n@phar.nagoya-cu.ac.jp

of the acetylated lysine substrate. Further, thiolate analogues showed potent cancer cell growth-inhibitory activities.^{20,21} Based on these findings, we designed FR-targeted prodrugs of HDAC inhibitors. Unlike hydroxamates and *o*-aminoanilides, such as SAHA and MS-275, thiolate HDAC inhibitors can be conjugated with a folic acid moiety via a disulfide bond, which would be reduced under reductive conditions, releasing the free thiol as an active species. We designed the folic acid-NCH-31 conjugates **1** and **2** (Fig. 2), which are expected to be recognized by the FR located on the cell surface, to enter cells via receptor-mediated endocytosis, and then to release the HDAC inhibitor NCH-31 upon cleavage of the disulfide bond in the cellular environment. We also designed the symmetrical disulfide **3** bearing a folic acid moiety. The reduced form of compound **3** itself could behave as an HDAC inhibitor.

The synthesis of the folic acid-NCH-31 conjugate **1** is outlined in Scheme 1. Mercaptoethylamine **4** was converted into 2-(2-(2-pyridinyl)disulfanyl)ethylamine **5** by the Boc protection of **4**, followed by treatment with 2,2'-dithiopyridine and Boc deprotection. Compound **5** was then coupled with *N*-Boc-L-glutamic acid α -*tert*-butyl ester to give the amide **6**. Treatment of compound **6** with NCH-31^{17,20} in DMF afforded the sulfur-exchanged product **7**. Universal deprotection of **7** using hydrochloric acid yielded the NCH-31-glutamic acid linked compound **8**. The folic acid-NCH-31 conjugate **1** was obtained in 92% yield by the reaction of **8** with pteroyl azide **9**²² in DMSO in the presence of tetramethylguanidine.

Scheme 2 shows the preparation of the other folic acid-NCH-31 conjugate **2**. Compound **2** was synthesized from 2,2'-(ethylenedioxy)diethylamine **10**. Reaction of the diamine **10** with an equivalent amount of (Boc)₂O gave the mono-Boc-protected compound **11**. Coupling between amine **11** and 3-mercaptopropanoic acid in the presence of EDCI and HOBT afforded **12**. The folic acid-NCH-31 conjugate **2** was prepared from the thiol **12** in the same manner as described for the synthesis of **1**.

The attempted route to **3** is shown in Scheme 3. In this scheme, we anticipated that disulfide dimer **3** would be

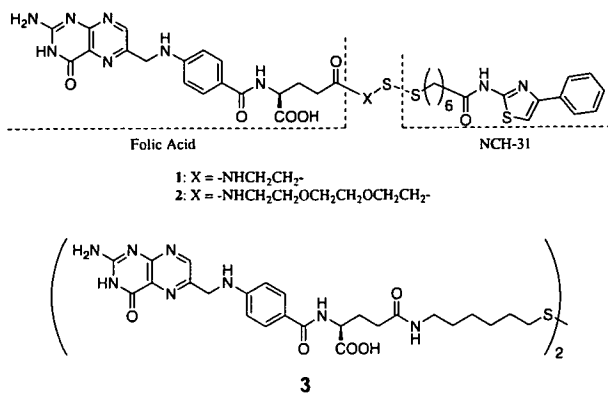
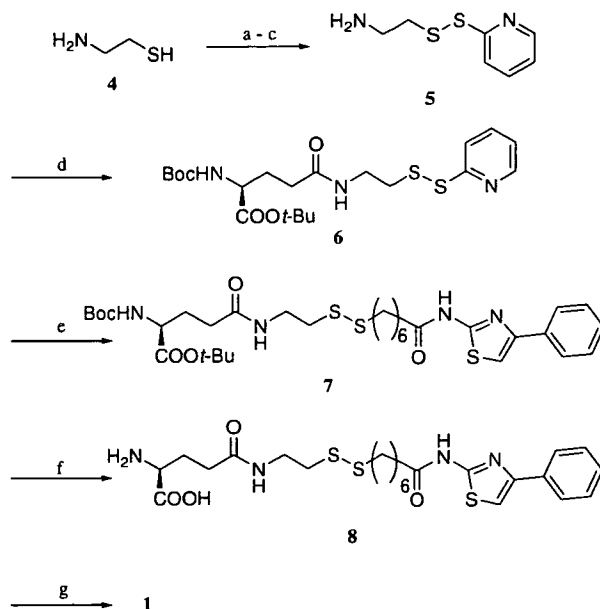
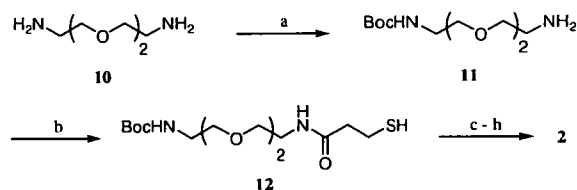


Figure 2. Candidate FR-targeted prodrugs of thiolate HDAC inhibitors.

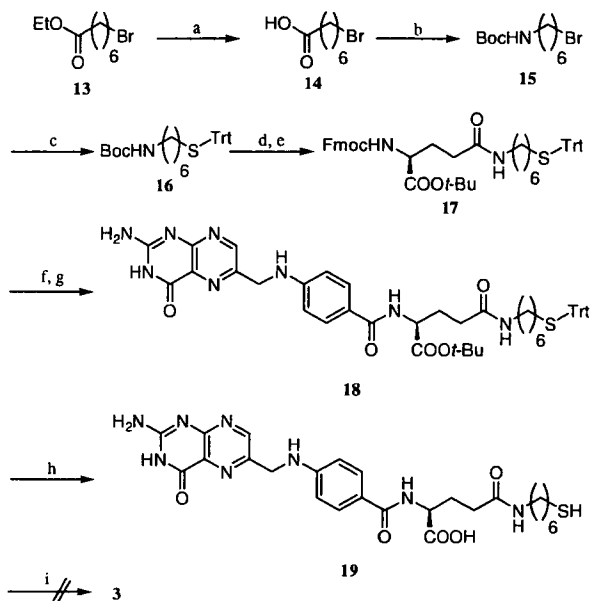


Scheme 1. Reagents and conditions: (a) (Boc)₂O, Et₃N, CH₂Cl₂, rt; (b) 2,2'-dithiopyridine MeOH, rt; (c) HCl, AcOEt, rt, 39% (three steps); (d) Boc-Glu-O-*t*-Bu, EDCI, HOBT, Et₃N, CH₂Cl₂, rt, 76%; (e) NCH-31, DMF, rt, 86%; (f) HCl, AcOEt, rt, quant; (g) pteroyl azide (**9**), tetramethylguanidine, DMSO, rt, 92%.



Scheme 2. Reagents and conditions: (a) (Boc)₂O, CH₂Cl₂, 0 °C to rt, quant; (b) 3-mercaptopropanoic acid, EDCI, HOBT, CH₂Cl₂, rt, 53%; (c) 2,2'-dithiopyridine MeOH, rt; (d) HCl, AcOEt, rt; (e) Boc-Glu-O-*t*-Bu, EDCI, HOBT, Et₃N, CH₂Cl₂, rt; (f) NCH-31, DMF, rt; (g) HCl, AcOEt, rt; (h) **9**, tetramethylguanidine, DMSO, rt, 59% (six steps).

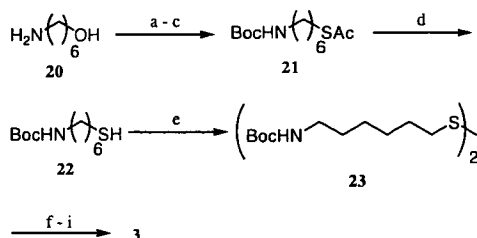
obtained from the corresponding thiol monomer by reaction with I₂. The 7-bromoheptanoic acid ethyl ester **13** was hydrolyzed to give the carboxylic acid **14**, after which Curtius rearrangement of the acyl azide prepared from **14** using diphenylphosphoryl azide (DPPA) provided the isocyanate. This, on treatment with *tert*-butanol, gave the *N*-Boc compound **15**. Treatment of **15** with triphenylmethanethiol in the presence of NaOMe afforded compound **16**. Deprotection of the Boc group of **16** and coupling with *N*-Fmoc-L-glutamic acid α -*tert*-butyl ester gave the amide **17**. The Fmoc group of **17** was removed using piperidine and coupling with pteroyl azide **9** afforded compound **18**. Removal of the *tert*-butyl group and the triphenylmethyl group of **18** under acidic conditions gave the thiol **19**. Although **19** was successfully obtained from **13** in eight steps, it was poorly soluble. We examined a variety of solvents for the dimerization of **19** using I₂, but a suspension of **19** with I₂ failed to provide the disulfide dimer **3**.



Scheme 3. Reagents and conditions: (a) LiOH, THF, EtOH, H₂O, rt, quant; (b) 1-DPPA, Et₃N, reflux, 2-*t*-BuOH, toluene, reflux, 44%; (c) NaOMe, HS-Trt, toluene, EtOH, 60 °C, 94%; (d) TFA, CH₂Cl₂, rt; (e) Fmoc-Glu-O-*t*-Bu, EDCI, HOBT, CH₂Cl₂, rt, 76% (two steps); (f) piperidine, DMF, rt, 87%; (g) **9**, tetramethylguanidine, DMSO, rt, 21%; (h) TFA, CH₂Cl₂, rt, 94%; (i) I₂.

We succeeded in obtaining **3** through the route outlined in Scheme 4. In this route, a disulfide bond was formed in the early stage. Initially, 6-aminohexanol **20** was converted to compound **21** by *N*-Boc protection, *O*-tosylation, and treatment with potassium thioacetate. The acetyl group of **21** was then removed to give the thiol **22**, and the disulfide dimer **23** was obtained by the reaction of the thiol monomer **22** with I₂. The desired disulfide **3** was successfully obtained from **23** in 74% yield using the same procedure as described for the synthesis of **1**.

Compounds **1–3** were initially tested in an *in vitro* HDAC inhibition assay under reductive conditions (Table 1).²³ Among these compounds, compound **1** showed the most potent activity inhibiting HDACs with an IC₅₀ of 0.27 μM, and the activity was comparable with that of NCH-31. This result suggested that the



Scheme 4. Reagents and conditions: (a) (Boc)₂O, THF, rt; (b) TsCl, Et₃N, THF, rt; (c) KSAc, acetone, rt, 75% (three steps); (d) aq NaOH, MeOH, THF, rt, 71%; (e) I₂, MeOH, rt, 95%; (f) HCl, AcOEt, rt; (g) Boc-Glu-O-*t*-Bu, EDCI, HOBT, Et₃N, CH₂Cl₂, rt; (h) HCl, AcOEt, rt; (i) **9**, tetramethylguanidine, DMSO, rt, 74% (four steps).

Table 1. HDAC inhibition data for NCH-31, **1–3**, and **19**^a

Entry	Compound	IC ₅₀ (μM)
1	NCH-31	0.17 ^b
2	1 ^c	0.27
3	2 ^c	3.0
4	3 ^c	9.0
5	19	21

^a Values are means of at least three experiments.

^b Data taken from the literature (Ref. 20).

^c Incubated with DTT (250 μM).

disulfide bond of compound **1** was reduced to release NCH-31 under the reductive conditions. On the other hand, the HDAC-inhibitory activities of compounds **2** and **3** were weaker than that of **1**. The reason for the weaker activity of **2** is unclear, but it may be because compound **2** is resistant to reduction as compared with compound **1**.

To confirm the effectiveness of the folic acid-based prodrugs of HDAC inhibitors, compounds **1** and **2** were tested in a cancer cell growth inhibition assay²⁴ using FR-positive human breast cancer MCF-7 cells.²⁵ Consistent with the results in the enzyme assay, compound **1** displayed dose-dependent cell growth-inhibitory activity (Fig. 3). Further, a competition experiment with 100 μM free folic acid significantly reduced the cell growth-inhibitory activity of **1**, demonstrating that the FR is responsible for the cellular entry of **1** (Fig. 4). In addition, treatment of MCF-7 cells with compound **1** produced an increase in the accumulation of acetylated histone H4 (Fig. 5),²⁶ which indicated that the cell growth-inhibitory activity of compound **1** significantly correlates with the inhibition of HDACs. Furthermore, the activity of **1** to cause histone hyperacetylation was significantly reduced by 100 μM free folic acid (Fig. 5). These results also suggested that the uptake of compound **1** is FR mediated.

In summary, we have designed and synthesized FR-targeted prodrugs of thiolate HDAC inhibitors that possess a cleavable disulfide bond. The folic acid-NCH-31 conjugate **1** showed potent HDAC-inhibitory activity under reductive conditions. Furthermore, compound **1** exerted growth-inhibitory activity against FR-positive breast cancer MCF-7 cells, and the cellular uptake of **1** was considered to be FR mediated, based on a competition experiment with free folic acid. Our strategy of utilizing

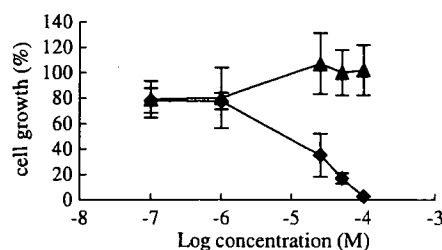


Figure 3. Growth inhibition of FR-positive MCF-7 cells by compounds **1** (●) and **2** (▲).

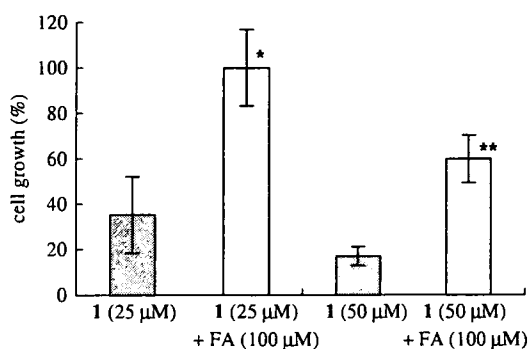


Figure 4. Growth inhibition of FR-positive MCF-7 cells by **1** and **1** plus 100 μM free folic acid (FA). * $p < 0.05$; ** $p < 0.01$ by Student's t test.

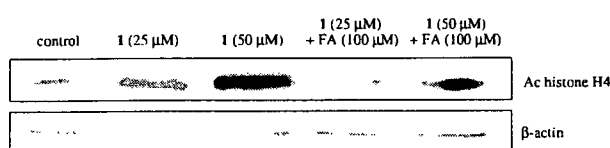


Figure 5. Western blot analysis of histone hyperacetylation in MCF-7 cells produced by **1** and **1** plus 100 μM free folic acid (FA).

a disulfide bond to connect a thiolate HDAC inhibitor with folic acid should be applicable to other anticancer agents bearing a thiol group, such as thiolate matrix metalloproteinase inhibitors²⁷ and thiolate farnesyltransferase inhibitors.²⁸ Our findings in this study provide the basis for a new approach to developing candidate antitumor agents with potentially fewer side effects.

Acknowledgments

This work was supported in part by Grants-in-Aid for Young Scientists (B) from the Ministry of Education, Science, Culture, Sports, Science, and Technology, Japan, and a grant from Takeda Science Foundation.

References and notes

- Miller, T. A.; Witter, D. J.; Belvedere, S. *J. Med. Chem.* **2003**, *46*, 5097.
- Miller, T. A. *Expert Opin. Ther. Pat.* **2004**, *14*, 791.
- Biel, M.; Wascholowski, V.; Giannis, A. *Angew. Chem. Int. Ed. Engl.* **2005**, *44*, 3186.
- Suzuki, T.; Miyata, N. *Curr. Med. Chem.* **2006**, *13*, 935.
- Richon, V. M.; Emiliani, S.; Verdin, E.; Webb, Y.; Breslow, R.; Rifkind, R. A.; Marks, P. A. *Proc. Natl. Acad. Sci. U.S.A.* **1998**, *95*, 3003.
- Saito, A.; Yamashita, T.; Mariko, Y.; Nosaka, Y.; Tsuchiya, K.; Ando, T.; Suzuki, T.; Tsuruno, T.; Nakanishi, O. *Proc. Natl. Acad. Sci. U.S.A.* **1999**, *96*, 4592.
- Kelly, W. K.; Richon, V. M.; O'Connor, O.; Curley, T.; MacGregor-Curtelli, B.; Tong, W.; Klang, M.; Schwartz, L.; Richardson, S.; Rosa, E.; Drobnjak, M.; Cordon-Cordo, C.; Chiao, J. H.; Rifkind, R.; Marks, P. A.; Scher, H. *Clin. Cancer Res.* **2003**, *9*, 3578.
- Kelly, W. K.; O'Connor, O. A.; Krug, L. M.; Chiao, J. H.; Heaney, M.; Curley, T.; MacGregore-Cortelli, B.; Tong, W.; Secrist, J. P.; Schwartz, L.; Richardson, S.; Chu, E.; Olgac, S.; Marks, P. A.; Scher, H.; Richon, V. M. *J. Clin. Oncol.* **2005**, *23*, 3923.
- Ryan, Q. C.; Headlee, D.; Acharya, M.; Sparreboom, A.; Trepel, J. B.; Ye, J.; Figg, W. D.; Hwang, K.; Chung, E. J.; Murgo, A.; Melillo, G.; Elsayed, Y.; Monga, M.; Kalnitskiy, M.; Zwiebel, J.; Sausville, E. A. *J. Clin. Oncol.* **2005**, *23*, 3912.
- Antony, A. C. *Blood* **1992**, *79*, 2807.
- Ross, J. F.; Chaudhuri, P. K.; Ratnam, M. *Cancer* **1994**, *73*, 2432.
- Weitman, S. D.; Lark, R. H.; Coney, L. R.; Fort, D. W.; Frasca, V.; Zurawski, V. R.; Kamen, B. A. *Cancer Res.* **1992**, *52*, 3396.
- Weitman, S. D.; Weinberg, A. G.; Coney, L. R.; Zurawski, V. R.; Jennings, D. S.; Kamen, B. A. *Cancer Res.* **1992**, *52*, 6708.
- Leamon, C. P.; Reddy, J. A. *Adv. Drug Deliv. Rev.* **2004**, *56*, 1143.
- Canevari, S.; Mezzanzanica, D.; Menard, S.; Ferrini, S.; Moretta, L.; Colnaghi, M. I. *Int. J. Cancer* **1992**, *7*, 42.
- Yamaguchi, T.; Tsurumi, H.; Kotani, T.; Yamaoka, N.; Otsuji, E.; Kitamura, K.; Takahashi, T. *Jpn. J. Cancer Res.* **1994**, *85*, 167.
- Suzuki, T.; Kouketsu, A.; Matsuura, A.; Kohara, A.; Ninomiya, S.; Kohda, K.; Miyata, N. *Bioorg. Med. Chem. Lett.* **2004**, *14*, 3313.
- Suzuki, T.; Matsuura, A.; Kouketsu, A.; Nakagawa, H.; Miyata, N. *Bioorg. Med. Chem. Lett.* **2005**, *15*, 331.
- Suzuki, T.; Kouketsu, A.; Itoh, Y.; Hisakawa, S.; Maeda, S.; Yoshida, M.; Nakagawa, H.; Miyata, N. *J. Med. Chem.* **2006**, *49*, 4809.
- Suzuki, T.; Nagano, Y.; Kouketsu, A.; Matsuura, A.; Maruyama, S.; Kurotaki, M.; Nakagawa, H.; Miyata, N. *J. Med. Chem.* **2005**, *48*, 1019.
- Suzuki, T.; Hisakawa, S.; Itoh, Y.; Maruyama, S.; Kurotaki, M.; Nakagawa, H.; Miyata, N. *Bioorg. Med. Chem. Lett.* **2007**, *17*, 1558.
- Luo, J.; Smith, M. D.; Lantrip, D. A.; Wang, S.; Fuchs, P. L. *J. Am. Chem. Soc.* **1997**, *119*, 10004.
- The HDAC activity assay was performed using an HDAC fluorescent activity assay/drug discovery kit (AK-500, BIOMOL Research Laboratories). HeLa Nuclear Extracts (0.5 μL/well) were incubated at 37 °C with 25 μM of Fluor de Lys™ substrate and various concentrations of samples. Reactions were stopped after 30 min by adding Fluor de Lys™ Developer with trichostatin A which stops further deacetylation. Then, 15 min after addition of this developer, the fluorescence of the wells was measured on a fluorometric reader with excitation set at 360 nm and emission detection set at 460 nm, and the % inhibition was calculated from the fluorescence readings of inhibited wells relative to those of control wells. The concentration of compound which results in 50% inhibition was determined by plotting the log[Inh] versus the logit function of the % inhibition. IC₅₀ values are determined using a regression analysis of the concentration/inhibition data.
- MCF-7 human breast cancer cells were purchased from American Type Culture Collection (ATCC, Manassas, VA, USA) and cultured in Dulbecco's modified Eagle's medium (DMEM) containing penicillin and streptomycin, which was supplemented with fetal bovine serum as described in the ATCC instructions. MCF-7 cells were plated in 96-well plates at initial densities of 5000 cells/well (50 μL/well) and incubated at 37 °C. After 24 h, cells were exposed to a solution of test compounds in DMEM (50 μL) at various concentrations in DMEM at 37 °C in

- 5% CO₂ for 72 h. Then, 10 μL of alamarBlue™ was added, and cells were incubated at 37 °C for 3 h. The fluorescence of the wells was measured on a fluorometric reader with excitation set at 530 nm and emission detection set at 590 nm, and the percentage of cell growth was calculated from the fluorescence readings.
25. Lee, E. S.; Na, K.; Bae, Y. H. *J. Control. Release* **2003**, *91*, 103.
 26. MCF-7 cells were cultured in DME culture medium containing penicillin and streptomycin, which was supplemented with fetal bovine serum as described in the ATCC instructions. MCF-7 cells (5×10^5) were treated for 14 h with samples at the indicated concentrations in 10% FBS-supplemented DMEM then collected and extracted with SDS buffer. Protein concentrations of the lysates were determined using a Bradford protein assay kit (Bio-Rad Laboratories); equivalent amounts of proteins from each lysate were resolved in 15% SDS–polyacrylamide gel and then transferred onto nitrocellulose membranes (Bio-Rad Laboratories). After blocking for 30 min with Tris-buffered saline (TBS) containing 3% skim milk, the transblotted membrane was incubated overnight at 4 °C with hyperacetylated histone H4 antibody (Upstate Biotechnology) (1:2000 dilution) or β-actin antibody (Abcam) (1:1000 dilution) in TBS containing 3% skim milk. After probing with the primary antibody, the membrane was washed twice with water, then incubated with goat anti-rabbit or anti-mouse IgG-horseradish peroxidase conjugates (diluted 1:5000) for 2 h at room temperature, and further washed twice with water. The immunoblots were visualized by enhanced chemiluminescence.
 27. Whittaker, M.; Floyd, C. D.; Brown, P.; Gearing, A. J. H. *Chem. Rev.* **1999**, *99*, 2735.
 28. Bell, I. M. *J. Med. Chem.* **2004**, *47*, 1869.



Phenylpropanoic acid derivatives bearing a benzothiazole ring as PPAR δ -selective agonists

Hiroki Fujieda,^a Shinya Usui,^a Takayoshi Suzuki,^a Hidehiko Nakagawa,^a
Michitaka Ogura,^b Makoto Makishima^b and Naoki Miyata^{a,*}

^aGraduate School of Pharmaceutical Sciences, Nagoya City University, 3-1 Tanabe-dori, Mizuho-ku, Nagoya, Aichi 467-8603, Japan

^bNihon University School of Medicine, 30-1 Oyaguchi-kamicho, Itabashi-ku, Tokyo 173-8610, Japan

Received 17 March 2007; revised 2 May 2007; accepted 8 May 2007

Available online 13 May 2007

Abstract—To find novel PPAR δ -selective agonists, we designed and synthesized phenylpropanoic acid derivatives bearing 6-substituted benzothiazoles. Optimization of this series led to the identification of a potent and selective PPAR δ agonist **17**. Molecular modeling suggested that compound **17** occupies the Y-shaped pocket of PPAR δ appropriately.

© 2007 Elsevier Ltd. All rights reserved.

Peroxisome proliferator-activated receptors (PPARs) are members of the nuclear receptor superfamily and the PPAR subfamily consists of three members, PPAR α , PPAR γ , and PPAR δ .¹ Many studies on PPAR α and PPAR γ have been performed and their roles are well established.^{2,3} Further, these efforts led to the discovery of hypolipidemic agents⁴ and insulin sensitizers.^{5,6} Meanwhile, the role of PPAR δ is just beginning to emerge. Several studies have suggested that PPAR δ plays an important role in regulating lipid metabolism and energy homeostasis in muscle and adipose tissues^{7–12} and the activation of PPAR δ increases HDL levels, attenuates weight gain, and improves insulin sensitivity.^{7,10} Thus, PPAR δ -selective agonists are of interest not only as tools for elucidating the more intricate biological functions of PPAR δ but also as candidate drugs for metabolic syndrome.

We previously reported compound **1** as a potent PPAR γ ligand¹³ and compound **2** as a potent PPAR α ligand^{14,15} (Fig. 1). In the course of our SAR studies on phenylpropanoic acid derivatives, we discovered that compound **4**, in which the pyridine ring of **1** is replaced by a benzothiazole ring, showed selective PPAR δ activity as compared with the other aromatic compounds **1**, **3**,

and **5**,¹⁵ although the activity was not so strong (Fig. 2). Since PPAR δ agonists having a benzothiazole ring have never been reported, we chose compound **4** as the lead compound for the exploration of novel PPAR δ -selective agonists. We describe here the design, synthesis, and PPAR δ selectivity of a series of phenylpropanoic acid derivatives bearing a 6-substituted benzothiazole ring.

The routes used for the synthesis of compounds **4–17** are illustrated in Schemes 1–5.

Preparation of compounds **3** and **4** is shown in Scheme 1. Ethyleneglycol **18** was allowed to react with *tert*-butyldimethylsilylchloride to give mono-alcohol **19**. Secondary amine **23**, the key intermediate for the preparation of **3** and **4**, was synthesized using a 2-nitrobenzenesulfonyl (nosyl) group^{16,17}: *n*-Nonylamine **20** was treated with 2-nitrobenzenesulfonylchloride to afford *N*-nosyl nonylamine **21**. Mitsunobu reaction was applied to the conversion of **21** into *N*-alkyl compound **22**.¹⁸ The nosyl group was removed by treating with benzenethiol in the presence of K₂CO₃ in anhydrous DMF to give a secondary amine **23**. Preparation of *N*-phenyloxazolyl compound **25a** and *N*-phenylthiazolyl compound **25b** was achieved by the method of Buchwald¹⁹: treatment of **23** with 2-chlorobenzoxazole or 2-chlorobenzothiazole **24**, Pd₂(DBA)₃, BINAP, and *tert*-BuONa in toluene. The TBS group of **25a** and **25b** was removed by treating with tetrabutylammonium fluoride (TBAF) in THF to give alcohols **26a** and **26b**,

Keywords: PPAR δ ; Agonist; Drug design; Nuclear receptor; Metabolic syndrome.

* Corresponding author. Tel.: +81 52 836 3407; fax: +81 52 836 3407; e-mail: miyata-n@phar.nagoya-cu.ac.jp

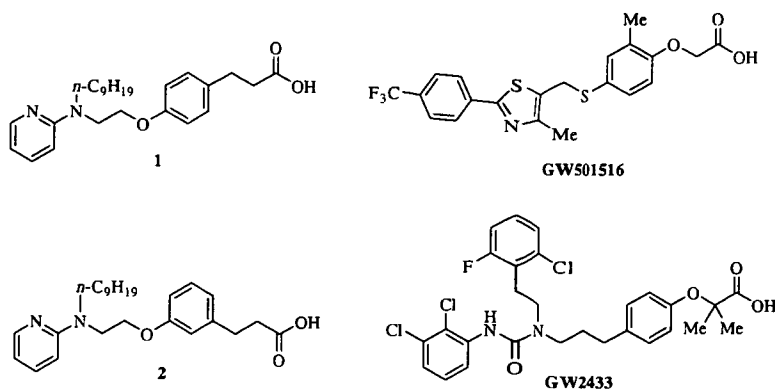


Figure 1. Structures of compounds 1 and 2, GW501516, and GW2433.

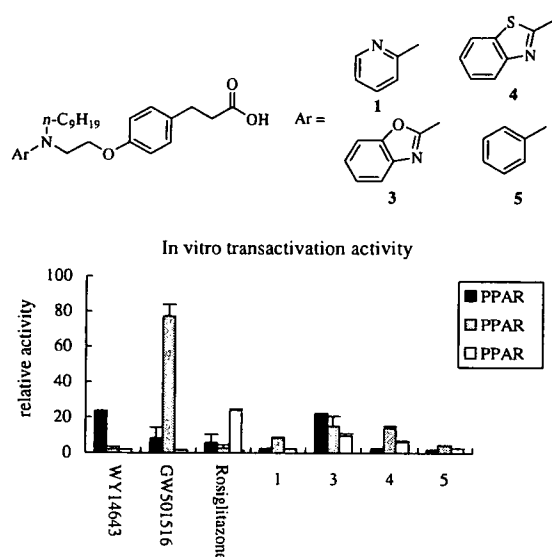
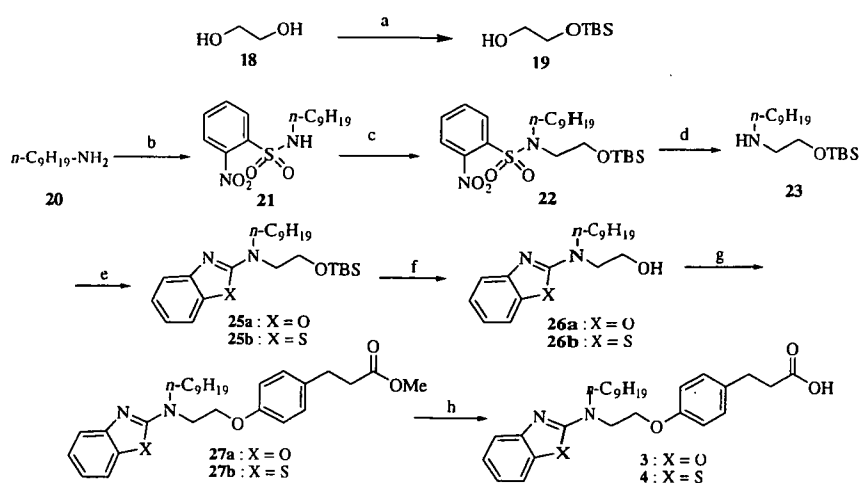


Figure 2. In vitro functional PPAR transactivation activity of compounds 1 and 3–5. WY14643 (PPAR α agonist) and GW501516 (PPAR δ agonist), Rosiglitazone (PPAR γ agonist) were used as reference compounds. GW501516 was used at 1 μ M and others at 10 μ M.

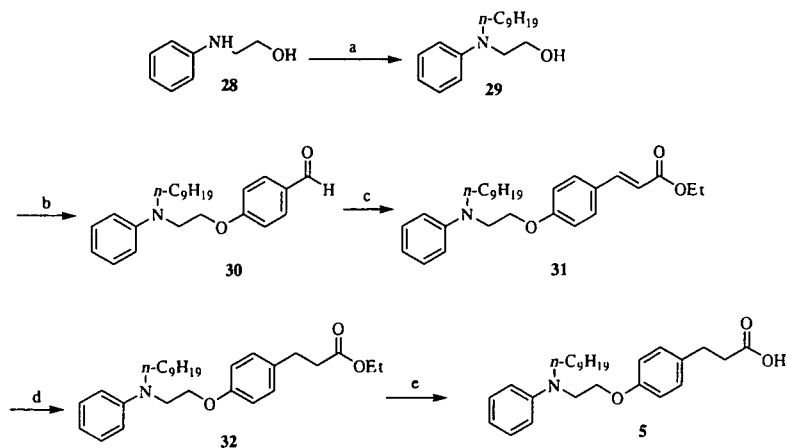
which were converted into ethers 27a and 27b by Mitsunobu reaction. Treatment of 27a and 27b with aqueous NaOH gave the desired carboxylic acids 3 and 4.

The preparation of compound 5 is outlined in Scheme 2. *N*-phenylaminoethanol 28 was allowed to react with 1-iodononane to give *N*-alkyl compound 29. Nucleophilic aromatic substitution by treatment of 29 with 4-fluorobenzaldehyde in the presence of sodium hydride gave ether 30. Conversion of aldehyde 30 into 31 was achieved by Horner–Wadsworth–Emmons reaction.²⁰ The double bond of 31 was hydrogenated and subsequent hydrolysis gave carboxylic acid 5.

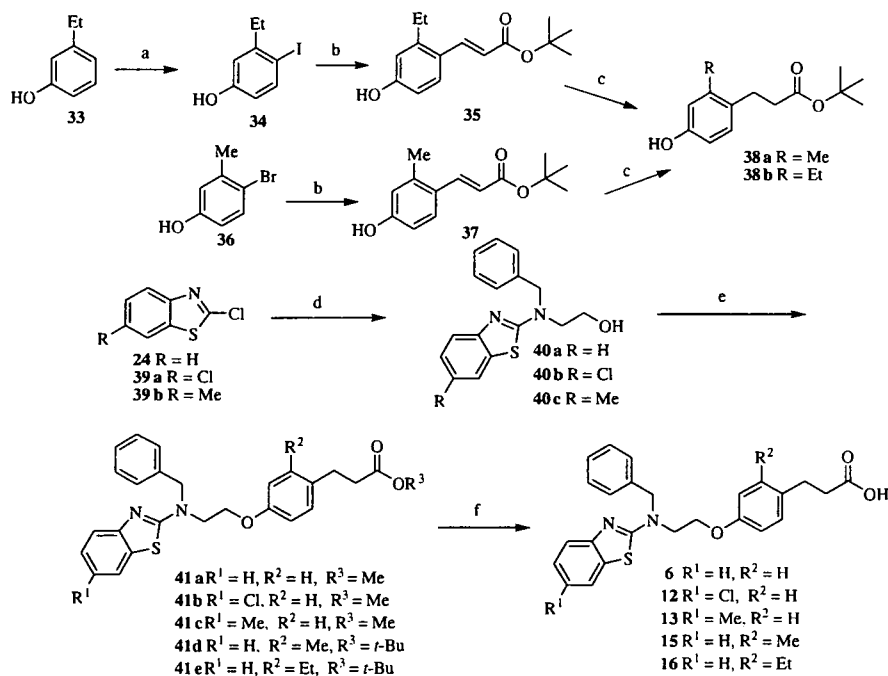
Preparation of compounds 6, 12, 13, 15, and 16 is shown in Scheme 3. 4-Bromo-3-ethylphenol 33 was allowed to react with KI, KIO₃, and HCl to give 4-iodo-3-ethylphenol 34.²¹ The Heck reaction was applied to the conversion of 34 into 35, and 36 into 37.²² Compounds 24, 39a, and 39b were allowed to react with *N*-benzylaminoethanol to give tertiary amines 40a–c. The conversion of 40a–c into 41a–e was achieved by Mitsunobu reaction, and subsequent hydrolysis or treatment with TFA afforded carboxylic acids 6, 12, 13, 15, and 16.



Scheme 1. Reagents and conditions: (a) *tert*-butyldimethylsilyl chloride, Et₃N, CH₂Cl₂, DMAP, rt, 75%; (b) 2-nitrobenzenesulfonyl chloride, K₂CO₃, CH₂Cl₂, rt, 93%; (c) 19, DEAD, PPh₃, anhydrous THF, 0 °C to rt; (d) benzenethiol, K₂CO₃, anhydrous DMF, rt, 83% (2 steps); (e) 2-chlorobenzoxazole or 2-chlorobenzothiazole (24), Pd₂(DBA)₃, rac-BINAP, *tert*-BuONa, anhydrous toluene, 105 °C; (f) TBAF, THF, rt, 62–67% (2 steps); (g) methyl 3-(4-hydroxyphenyl)propionate, DEAD, PPh₃, anhydrous THF, 0 °C to rt, 70–72%; (h) 2 N aq NaOH, MeOH, THF, rt, 99–100%.



Scheme 2. Reagents and conditions: (a) 1-iodononane, 1,4-dioxane, 100 °C, 81%; (b) i—NaH, anhydrous DMF, 0 °C to 50 °C, ii—4-fluorobenzaldehyde, anhydrous DMF, rt, 26%; (c) (EtO)₂P(O)CH₂CO₂Et, NaH, anhydrous THF, 0 °C to rt, 42%; (d) H₂, Pd/C, MeOH, rt, 79%; (e) 2 N aq NaOH, EtOH–THF, rt, 97%.

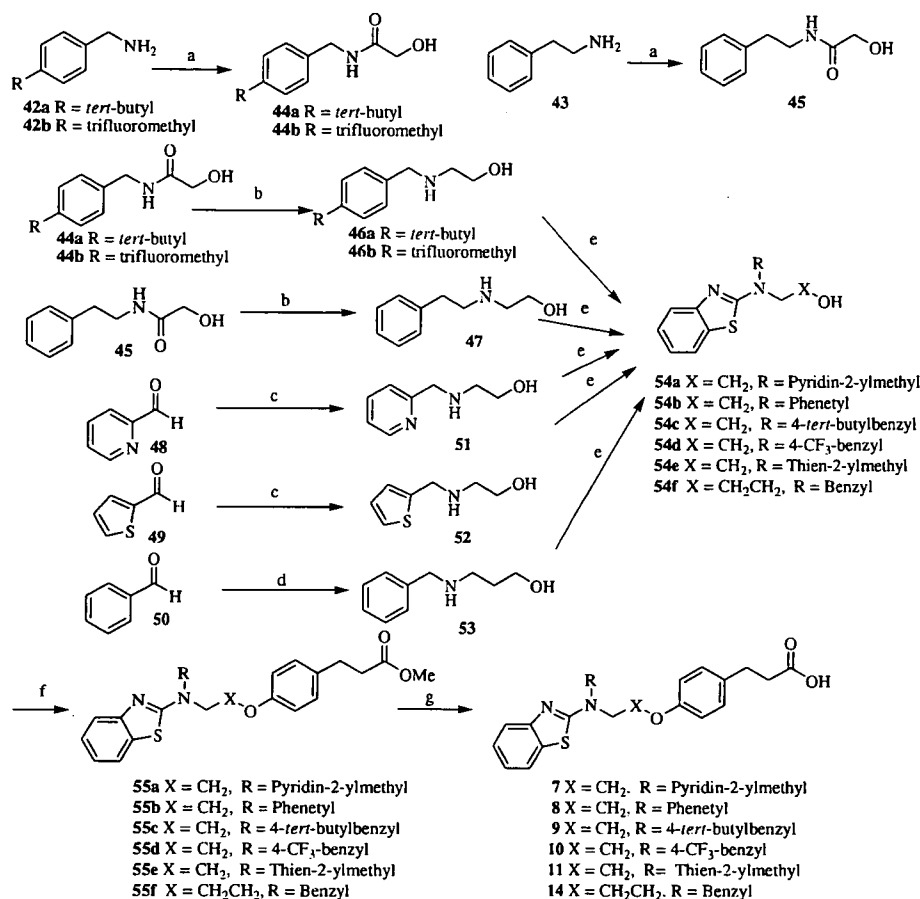


Scheme 3. Reagents and conditions: (a) KI, KIO₃, HCl, 60%; (b) *tert*-butylacrylate, Pd(OAc)₂, P(*o*-tol)₃, Et₃N, 110 °C, 58–83%; (c) H₂, Pd/C, MeOH, rt, 75–81%; (d) *N*-benzylaminoethanol, Pd₂(DBA)₃, rac-BINAP, *tert*-BuONa, anhydrous toluene, 80 °C or *N*-benzylaminoethanol, Et₃N, 100 °C, 44–79%; (e) methyl 3-(4-hydroxyphenyl)propionate or 38a or 38b, DEAD, PPh₃, anhydrous THF, 0 °C to rt, 24–77%; (f) 2 N aq NaOH, EtOH, THF, rt or TFA, CH₂Cl₂, rt, 22–81%.

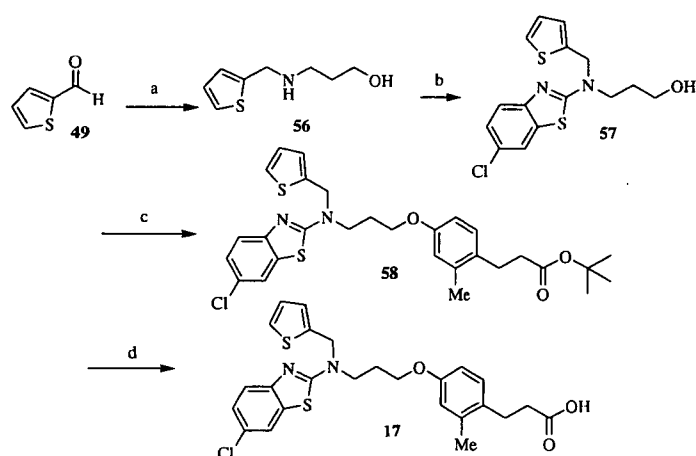
Compounds 7–11 and 14 were prepared as shown in Scheme 4. Coupling between glycolic acid and amines 42a, 42b, and 43 afforded amides 44a, 44b, and 45. Amides 44a, 44b, and 45 were reduced by LiAlH₄ to give secondary amines 46a, 46b, and 47. Reductive aminoalkylation of 2-aminoethanol or 3-amino-1-propanol with 48–50 gave secondary amines 51, 52, and 53. Amines 46a, 46b, 47, and 51–53 were allowed to react with 2-chlorobenzothiazole 24 to give tertiary

amines 54a–f. Alcohols 54a–f were converted into 7–11 and 14 in the same way as described for the synthesis of 3 and 4.

Preparation of compound 17 is shown in Scheme 5. Reductive aminoalkylation of 3-amino-1-propanol with aldehyde 49 gave 56. Amine 56 was converted to compound 17 by the same method described for the preparation of 15 and 16.



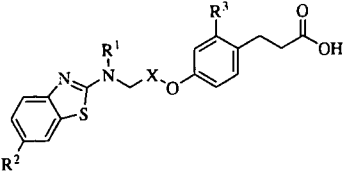
Scheme 4. Reagents and conditions: (a) glycolic acid, EDCI, DMAP, THF, rt, 51–73%; (b) LiAlH₄, anhydrous THF, 0 °C to reflux; (c) 2-aminoethanol, anhydrous MeOH, 0 °C, NaBH₄; (d) 1-amino-3-propanol, anhydrous MeOH, 0 °C, NaBH₄; (e) 2-chlorobenzothiazole, Et₃N, 100 °C, 10–30% (2 steps); (f) methyl 3-(4-hydroxyphenyl)propionate, DEAD, PPh₃, anhydrous THF, 0 °C to rt, 36–96%; (g) 2 N aq NaOH, EtOH, THF, rt, 15–80%.



Scheme 5. Reagents and conditions: (a) 3-amino-1-propanol, MeOH, NaBH₄; (b) 2,6-dichlorobenzothiazole, Et₃N, 100 °C, 83% (2 steps); (c) 38a, DEAD, PPh₃, anhydrous THF, 0 °C to rt, 64%; (d) TFA, CH₂Cl₂, rt, 73%.

Compounds 6–17 were tested in an *in vitro* transactivation assay against human PPAR subtypes and the results are listed in Table 1^{23,24}. GW501516 (Fig. 1) was used as a reference compound.

In previous reports, the co-crystal structure of PPAR δ with pan-agonist GW2433 (Fig. 1) has revealed that PPAR δ has a unique Y-shaped pocket and GW2433 fills all three legs of the pocket.^{25,26} The crystal structure also

Table 1. In vitro functional PPAR transactivation activity of compounds 4 and 6–17


Compound	X	R ¹	R ²	R ³	EC ₅₀ ^a		
					α (μM)	δ (μM)	γ (μM)
4	CH ₂	<i>n</i> -C ₉ H ₁₉	H	H	N.E. ^b	N.E. ^b	N.E. ^b
6	CH ₂	Benzyl	H	H	N.E. ^b	2.81	N.E. ^b
7	CH ₂	Pyridin-2-ylmethyl	H	H	N.E. ^b	N.E. ^b	N.E. ^b
8	CH ₂	Phenethyl	H	H	N.E. ^b	N.E. ^b	N.E. ^b
9	CH ₂	4- <i>tert</i> -Butylbenzyl	H	H	N.E. ^b	4.88	6.34
10	CH ₂	4-CF ₃ -benzyl	H	H	4.46	0.94	3.69
11	CH ₂	Thien-2-ylmethyl	H	H	N.E. ^b	1.74	N.E. ^b
12	CH ₂	Benzyl	Cl	H	N.E. ^b	1.36	N.E. ^b
13	CH ₂	Benzyl	Me	H	N.E. ^b	2.61	N.E. ^b
14	CH ₂ CH ₂	Benzyl	H	H	N.E. ^b	2.55	N.E. ^b
15	CH ₂	Benzyl	H	Me	N.E. ^b	1.17	N.E. ^b
16	CH ₂	Benzyl	H	Et	N.E. ^b	2.97	N.E. ^b
17	CH ₂ CH ₂	Thien-2-ylmethyl	Cl	Me	N.E. ^b	0.39	N.E. ^b
GW501516					N.E. ^c	0.085	N.E. ^c

^a Compounds were screened for agonist activity on PPAR-GAL4 chimeric receptors in transiently transfected HEK-293 cells as described. EC₅₀ value is the molar concentration of the test compound that affords 50% of maximal reporter activity.

^b N.E., did not have sufficient activity to determine EC₅₀ values up to 20 μM.

^c N.E., did not have sufficient activity to determine EC₅₀ values up to 10 μM.

made it clear that the two legs of the Y-shaped pocket are formed by hydrophobic amino acid residues and are not so large when compared with the hydrophobic regions of PPARα and PPARγ where the nonyl groups of compound 1 or compound 2 are estimated to be located.^{13,14} Based on these information, compounds 6–11 in which the nonyl group of 4 is replaced by smaller lipophilic groups were designed and synthesized. Since

compounds 6–11 could possibly have Y-shaped conformation and lack a long alkylchain which is needed for affinity to PPARα or PPARγ,^{13,14} they were expected to bind PPARδ selectively. As shown in Table 1, compound 6 (R¹ = Bn), compound 9 (R¹ = 4-*tert*-butylbenzyl), compound 10 (R¹ = 4-CF₃-benzyl), and compound 11 (R¹ = thien-2-ylmethyl) were found to be PPARδ agonists more potent than lead compound 4,

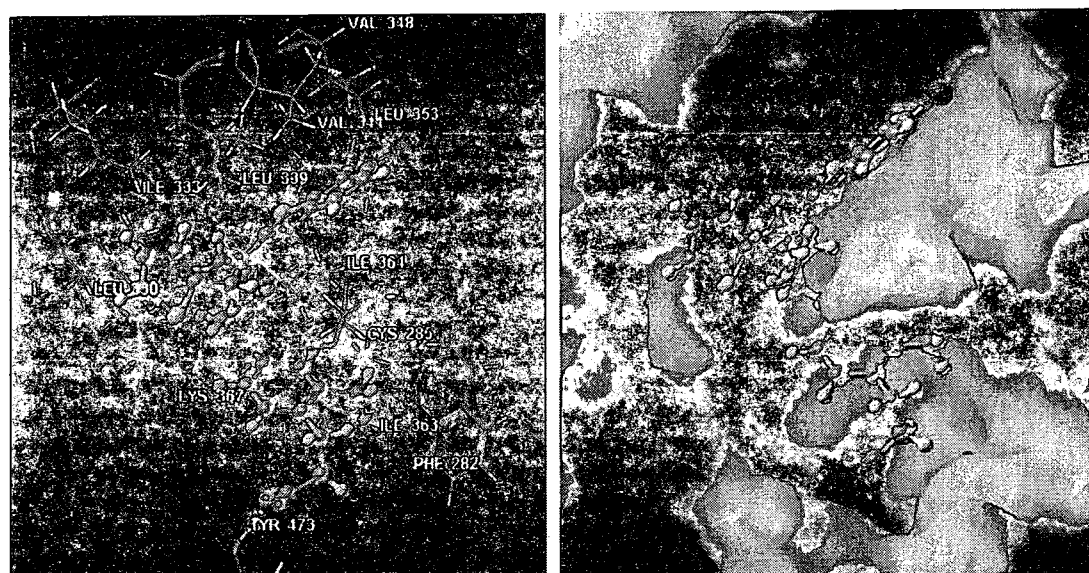


Figure 3. View of the conformation of 17 docked in PPARδ. Amino acid residues and hydrogen bonds are displayed as wires and dotted lines, respectively (left), and the surface of the PPARδ is displayed in the background (right).

and compounds **6** and **11** also showed selectivity towards PPAR δ .

Having investigated the requirements for the R¹ group, we next turned our attention to the benzothiazole ring. The R¹ group was fixed as the benzyl group and the effect of a substituent at the 6-position of the benzothiazole ring (R² group) was examined. Among compounds **6**, **12**, and **13**, compound **12** (R² = Cl) showed transcriptional activity for PPAR δ more potently than compound **6**, whereas methyl compound **13** displayed activity similar to **6**.

We also examined the effect of linker length. Compound **14**, where X = CH₂CH₂, modestly improved the PPAR δ activity of compound **6**, where X = CH₂.

Since earlier studies revealed that the introduction of a methyl group at the *ortho* position of phenylpropanoic acid improved potency and selectivity toward PPAR δ ,^{26,27} we looked at the effects of the R³ group. The introduction of a methyl substituent at the *ortho* position of phenylpropanoic acid led to a 2.5-fold increase of PPAR δ activity (**6** vs **15**). On the other hand, the introduction of ethyl substitution (compound **16**) was not effective.

Encouraged by these findings, we prepared compound **17** with the best combination of R¹–R³ and X groups in this study. To our satisfaction, compound **17** showed the highest activity and selectivity for PPAR δ in this series.²⁸

Next, we studied the binding mode of compound **17**, the most active compound in this study, using Glide 3.5 and MacroModel 8.1 software.²⁹ As expected, inspection of the simulated PPAR δ /17 complex suggested that compound **17** had a Y-shaped conformation and filled the Y-shaped pocket of PPAR δ appropriately (Fig. 3). Specifically, the 6-Cl-benzothiazole ring and the thiophene ring are estimated to occupy each of the two legs of the Y-shaped pocket which are formed by Val 341, Cys, 285, Val 348 and by Leu 330, Ile 333, Leu 339, respectively. In addition, it was shown that the Me group of **17** is located in the small hydrophobic pocket composed of Phe 282, Cys 285, and Ile 363. Interestingly, a hydrogen bond was observed between the oxygen atom of the ether linker and Lys 367. This hydrogen bond may be another important factor for PPAR δ selectivity, because no such hydrogen bond has been observed between phenylpropanoic acid derivatives and PPAR α or PPAR γ .^{13,14,30}

In summary, to explore novel PPAR δ -selective agonists, we designed and prepared a series of phenylpropanoic acid derivatives. Compound **6** bearing a benzothiazole ring and a benzyl group showed PPAR δ activity and selectivity. The introduction of a Cl group at the C-6 position of the benzothiazole ring and Me group at the *ortho* position of phenylpropanoic acid further improved PPAR δ transcriptional activity. Compound **17**, which has the best R¹–R³ and X groups, was found to be the most potent and selective PPAR δ agonist in this series. Molecular modeling suggested that com-

ound **17** fills the Y-shaped pocket of PPAR δ appropriately. Currently, further detailed studies pertaining to compound **17** are under way.

References and notes

- Willson, T. M.; Brown, P. J.; Sternbach, D. D.; Henke, B. R. *J. Med. Chem.* **2000**, *43*, 527.
- Staels, B.; Dallongeville, J.; Auwerx, J.; Schoonjans, E.; Leitersdorf, E.; Fruchart, J.-C. *Circulation* **1998**, *98*, 2088.
- Way, J. M.; Harrington, W. W.; Brown, K. K.; Gottschalk, W. K.; Sundseth, S. S.; Mansfield, T. A.; Ramachandran, R. K.; Willson, T. M.; Klierer, S. A. *Endocrinology* **2001**, *142*, 1269.
- Forman, B. M.; Chen, J.; Evans, R. M. *Proc. Natl. Acad. Sci. U.S.A.* **1997**, *94*, 4312.
- Cantello, B. C. C.; Cawthorone, M. A.; Cottam, G. P.; Duff, P. T.; Haigh, D.; Hindley, R. M.; Lister, C. A.; Smith, S. A.; Thurlby, P. L. *J. Med. Chem.* **1994**, *37*, 3977.
- Momose, Y.; Meguro, K.; Ikeda, H.; Hatanaka, C.; Oi, S.; Sohda, T. *Chem. Pharm. Bull.* **1991**, *39*, 1440.
- Wang, Y.-X.; Lee, C.-H.; Tiep, S.; Yu, R. T.; Ham, J.; Kang, H.; Evans, R. M. *Cell* **2003**, *113*, 159.
- Wang, Y.-X.; Zhang, C.-L.; Yu, R. T.; Cho, H. K.; Nelson, M. C.; Bayuga-Ocampo, C. R.; Ham, J.; Kang, H.; Evans, R. M. *PLoS Biol.* **2004**, *2*, 1532.
- Leibowitz, M. D.; Fievet, C.; Hennuyer, N.; Peinado-Onsurbe, J.; Duez, H.; Berger, J.; Cullinan, C. A.; Sparrow, C. P.; Baffic, J.; Berger, G. D.; Santini, C.; Marquis, R. W.; Tolman, R. L.; Smith, R. G.; Moller, D. E.; Auwerx, J. *FEBS Lett.* **2000**, *473*, 333.
- Tanaka, T.; Yamamoto, J.; Iwasaki, S.; Asaba, H.; Hamura, H.; Ikeda, Y.; Watanabe, M.; Magoori, K.; Ioka, R. X.; Tachibana, K.; Watanabe, Y.; Uchiyama, Y.; Sumi, K.; Iguchi, H.; Ito, S.; Doi, T.; Hamakubo, T.; Naito, M.; Auwerx, J.; Yanagisawa, M.; Kodama, T.; Sakai, J. *Proc. Natl. Acad. Sci. U.S.A.* **2003**, *100*, 15924.
- Graham, T. L.; Mookherjee, C.; Suckling, K. E.; Palmer, C. N. A.; Patel, L. *Atherosclerosis* **2005**, *181*, 29.
- Lee, C.-H.; Chawla, A.; Urbiztondo, N.; Liao, D.; Boisvert, W. A.; Evans, R. M. *Science* **2003**, *302*, 453.
- Although compound **1** showed weak transactivation activity for PPAR γ (Fig. 2), it displayed high affinity to PPAR γ in a binding assay (Ref. 14,15).
- Usui, S.; Suzuki, T.; Hattori, Y.; Etoh, K.; Fujieda, H.; Nishizuka, M.; Imagawa, M.; Nakagawa, H.; Kohda, K.; Miyata, N. *Bioorg. Med. Chem. Lett.* **2005**, *15*, 1547.
- Usui, S.; Fujieda, H.; Suzuki, T.; Yoshida, N.; Nakagawa, H.; Miyata, N. *Bioorg. Med. Chem. Lett.* **2006**, *16*, 3249.
- Fukuyama, T.; Jow, C.-K.; Cheung, M. *Tetrahedron Lett.* **1995**, *36*, 6373.
- Fukuyama, T.; Cheung, M.; Jow, C.-K.; Hidai, Y.; Kan, T. *Tetrahedron Lett.* **1997**, *38*, 5831.
- Mitsunobu, O. *Synthesis* **1981**, 1.
- Wagaw, S.; Buchwald, S. L. *J. Org. Chem.* **1996**, *61*, 7240.
- Maryanoff, B. E.; Reitz, A. B. *Chem. Rev.* **1989**, *89*, 863.
- Li, T.; Fujita, Y.; Tsuda, Y.; Miyazaki, A.; Ambo, A.; Sasaki, Y.; Jinsmaa, Y.; Bryant, S. D.; Lazarus, L. H.; Okada, Y. *J. Med. Chem.* **2005**, *48*, 586.
- Beletskaya, I. P.; Cheprakov, A. V. *Chem. Rev.* **2000**, *100*, 3009.
- Fukuen, S.; Iwaki, M.; Yasui, A.; Makishima, M.; Matsuda, M.; Shimomura, I. *J. Biol. Chem.* **2005**, *280*, 23653.
- Human embryonic kidney (HEK) 293 cells were cultured in DMEM containing 5% fetal bovine serum at 37 °C in a humidified atmosphere of 5% CO₂ in air. Transfections of PPAR and reporter gene con-

- structs were performed by calcium phosphate coprecipitation. Eight hours after transfection, ligands were added. Cells were harvested 12–16 h after treatment, and luciferase and β -galactosidase activities were assayed using a 1420 ARVOTM MX multilabel counter (Perkin-Elmer, Boston, MA, U.S.A.). DNA cotransfection experiments included 58 ng of reporter plasmid, 12 ng of CMX- β -galactosidase, and 18 ng of each receptor expression plasmid per well in a 96-well plate. Luciferase data were normalized to an internal β -galactosidase control and reported values are means of triplicate assays.
25. Xu, H. E.; Lambert, M. H.; Montana, V. G.; Parks, D. J.; Blanchard, S. G.; Brown, P. J.; Sternbach, D. D.; Lehmann, J. M.; Wisely, G. B.; Willson, T. M.; Kliewer, S. A.; Milburn, M. V. *Mol. Cell* **1999**, *3*, 397.
 26. Epple, R.; Azimioara, M.; Russo, R.; Bursulaya, B.; Tian, S.-S.; Gerken, A.; Iskandar, M. *Bioorg. Med. Chem. Lett.* **2006**, *16*, 2969.
 27. Weigand, S.; Bischoff, H.; Dittrich-Wengenroth, E.; Heckroth, H.; Lang, D.; Vaupel, A.; Woltering, M. *Bioorg. Med. Chem. Lett.* **2005**, *15*, 4619.
 28. The relative efficacy of compound **17** was 86% of that of GW501516.
 29. The X-ray structure of PPAR δ complexed with GW2433 (PDB code 1GWX) was used as the target structure for docking. Protein preparation, receptor grid generation and ligand docking were performed using the software Glide 3.5. Compound **17** was docked into the ligand binding site of PPAR δ . The extra precision mode of Glide was used to determine favorable binding poses, which allowed the ligand conformation to be flexibly explored while holding the protein as a rigid structure during docking. The predicted complex structure was then fully energy-minimized with both the protein and the ligand allowed to move using Macromodel 8.1 software. The conformation of **17** in the PPAR δ ligand binding site was minimized by MM calculation based upon the OPLS-AA force field with each parameter set as follows; solvent: water, method: LBFGS, Max # Iterations: 10,000, Converge on: Gradient, Convergence Threshold: 0.05.
 30. Gampe, R. T., Jr.; Montana, V. G.; Lambert, M. H.; Miller, A. B.; Bledsoe, R. K.; Milburn, M. V.; Kliewer, S. A.; Willson, T. M.; Xu, H. E. *Mol. Cell* **2000**, *5*, 545.

Highlighted paper selected by Editor-in-chief

Nitration of Specific Tyrosine Residues of Cytochrome c Is Associated with Caspase-Cascade Inactivation

Hidehiko NAKAGAWA,^{*,a} Nobuko KOMAI,^b Mitsuko TAKUSAGAWA,^b Yuri MIURA,^c Tosifusa TODA,^c Naoki MIYATA,^a Toshihiko OZAWA,^b and Nobuo IKOTA^b

^aDepartment of Organic and Medicinal Chemistry, Graduate School of Pharmaceutical Sciences, Nagoya City University; Nagoya 467-8603, Japan; ^bRedox Regulation Research Group, National Institute of Radiological Sciences; Chiba 263-8555, Japan; and ^cTokyo Metropolitan Institute of Gerontology; Tokyo 173-0015, Japan.

Received August 10, 2006; accepted October 17, 2006; published online October 19, 2006

Peroxynitrite, a potent oxidative stress inducer, inhibits the mitochondrial electron transfer, induces cell death, and is considered to be involved in the pathology of various diseases. However, the intracellular mechanisms involved in the cell death process are not fully understood. Here we demonstrate that the enhanced nitration of specific tyrosine residues of cytochrome c, which are induced by continuous peroxynitrite exposure, attenuates cytochrome c-induced caspase-9 activation *in vitro*. Interestingly, cytochrome c nitrated with a single high dose of peroxynitrite preserved its potency, while this did not occur when cytochrome c was treated with continuous peroxynitrite exposure. Although both of these experiments resulted in cytochrome c nitration at the tyrosine residues, it was found that nitration at specific residues was enhanced only when cytochrome c was exposed to continuous peroxynitrite. This is the first report to demonstrate that cytochrome c nitration affects the apoptotic pathway by means of enhancement of nitration at specific tyrosine residues. This result implies that the nitration pattern of cytochrome c may affect the efficacy of the mitochondrial pathway in apoptotic cell death.

Key words cytochrome c; nitrotyrosine; apoptosis; peroxynitrite; caspase

Peroxynitrite is a very strong oxidant, and is considered a candidate as an *in vivo* oxidant for inducing the oxidative and “nitrative” stress in various diseases, such as cardiovascular disease,^{1–3} brain ischemia,^{4–7} Parkinson’s disease,^{8–10} Alzheimer’s disease,^{11–14} amyotrophic lateral sclerosis,^{15,16} other neurodegenerative diseases,^{17,18} and sepsis.^{19,20} Peroxynitrite causes nitration of free tyrosine and protein tyrosine residues. Although this reaction has been considered as the “footprint” of peroxynitrite production, it is not exclusively caused by peroxynitrite, but formed by the reaction of nitrite with hydrogen peroxide in the presence of myeloperoxidase.²¹ Nonetheless, protein tyrosine nitration is a clue that reactive nitrogen species (RNS), like peroxynitrite and its equivalents, are produced and that the biological system has been damaged by RNS stresses. Some reports indicate that the nitration of protein tyrosine residues can cause some changes in function. Radi and colleagues reported that cytochrome c was nitrated at a specific tyrosine residue by a bolus peroxynitrite treatment depending on the concentration of peroxynitrite.²² According to their results, nitration of cytochrome c resulted in loss of function as an ascorbate oxidase and in the downregulation of the oxygen consumption in mitochondrial preparation. We also independently reported that the nitration of a single tyrosine residue in cytochrome c by a relatively low dose of peroxynitrite resulted in the up-regulation of its peroxidase activity for hydrogen peroxide and in the actual impairment of the membrane potential formation, which is important for ATP synthesis, in isolated mitochondrial preparations.²³

It is well known that cytochrome c plays an important role in mitochondria-dependent apoptotic cell death. As a response to apoptotic stimuli, cytochrome c is released from the intermembrane space to the cytosol, and forms the apoptosome complex with procaspase-9 and Apaf-1 to activate caspase-9 and the downstream caspases, resulting in apop-

totic death execution. One report²⁴) investigated the effect of cytochrome c treated with a bolus of peroxynitrite on the apoptotic cascades. In that report, cytochrome c nitrated with a bolus treatment of peroxynitrite retained its ability for caspase activation. Under the pathophysiological conditions, however, peroxynitrite production was assumed to be relatively low and sustained. The effect of low-dose and continuous exposure of cytochrome c to peroxynitrite on caspase activation was not evaluated, and the relationship between cytochrome c nitration and the caspase cascade activation has not been well investigated.

Here, we report on the nitration of cytochrome c by various methods of peroxynitrite exposure, and we analyze the relationship between tyrosine nitration and the ability of cytochrome c to cause caspase cascade activation *in vitro*. We determined that the modification pattern of cytochrome c was dependent on the duration and concentration of peroxynitrite exposure, and that cytochrome c nitration by continuous exposure to peroxynitrite attenuated its potency for caspase 9 activation. However, cytochrome c nitration by a bolus peroxynitrite treatment did not change that ability.

MATERIALS AND METHODS

Chemicals Cytochrome c (bovine heart), aprotinin, and pepstatin A were purchased from Sigma (St. Louis, MO, U.S.A.). Pronase was from Boehringer-Mannheim (Mannheim, Germany). 3-Nitro-L-tyrosine, 5-methoxytryptamine and tetranitromethane (TNM) were from Aldrich (Milwaukee, WI, U.S.A.). Staurosporine and leupeptin were purchased from Wako Pure Chemical Industries Ltd. (Osaka, Japan). PMSF was from Nacalai Tesque (Kyoto, Japan). 3-Morpholinolinosydnonimine (SIN-1) was from Dojindo (Kumamoto, Japan). All other reagents were from Sigma, Bio-Rad (Hercules, CA, U.S.A.), or Amersham Biosciences

Corp. (Piscataway, NJ, U.S.A.) All the reagents were of analytical or biochemical grade.

Peroxynitrite Preparation Peroxynitrite was synthesized as an alkaline solution based on the method of Pryor *et al.*^{23,25} The solution was stored at -80°C until use. The concentration of the peroxynitrite solution was determined spectrophotometrically by measuring the absorbance at 302 nm ($\epsilon=1670\text{M}^{-1}\text{cm}^{-1}$). Using this method, up to a 500 mM solution of peroxynitrite was obtained. The concentration of the stock solution was determined again before use, and then the stock was diluted to the desired concentration with 0.01 M NaOH on an ice bath.

Cell Culture A C6 rat glioma cell line was purchased from American Type Culture Collection (ATCC, Manassas, VA, U.S.A.) and cultured in Ham's F10 medium containing penicillin and streptomycin, supplemented with horse serum and fetal bovine serum as described in the ATCC instruction. The cells were maintained at 37°C in a humidified 5% (v/v) CO_2 incubator under a sub-confluent condition.

Preparation of Peroxynitrite- and TNM-Treated Cytochrome c Cytochrome c solution ($20\ \mu\text{M}$) was prepared in PBS. For continuous treatment with peroxynitrite, $1\ \mu\text{l}$ of 50 mM peroxynitrite in 0.01 M NaOH was repeatedly added to 1 ml of the cytochrome c solution ($20\ \mu\text{M}$) 20 times at 30-s intervals while mixing. Because peroxynitrite is unstable and reactive at neutral pH, it is practically fully reacted or decomposed within 30 s after addition. For a continuous infusion, $20\ \mu\text{l}$ of 50 mM peroxynitrite in 0.01 M NaOH was continuously infused into 1 ml of the cytochrome c solution over 20 min with a syringe pump while mixing. For a single treatment with peroxynitrite, $20\ \mu\text{l}$ of 50 mM peroxynitrite was added to the cytochrome c solution all at once. For a low-dose single or control treatment, $1\ \mu\text{l}$ of 50 mM peroxynitrite or no peroxynitrite was added to the cytochrome c solution containing decomposed peroxynitrite equivalent to the $19\ \mu\text{l}$ or $20\ \mu\text{l}$ of 50 mM peroxynitrite, respectively. After the addition of $20\ \mu\text{l}$ of peroxynitrite solution, the resulting solution was confirmed to be neutral (pH 7 to 8). All the peroxynitrite-treated cytochrome c solutions were subjected to gel filtration with Sephadex G-25, or centrifugal concentration and wash with a membrane filter (polyethylenesulfonate, 5000 molecular weight cut off, Vivascience AG, Hanover, Germany). The cytochrome c concentrations were adjusted according to the absorbance at 409 nm. With the peroxynitrite treatment at the concentration range in these experiments, the maximum absorbance and wavelength of the Soret band (409 nm) showed almost no changes. The Soret band was slightly blue-shifted by less than 1 nm in wavelength. A solution of cytochrome c repeatedly treated with low-dose peroxynitrite in the presence of 5-methoxytryptamine (5MT) was also prepared in order to determine the inhibitory effect of 5MT.

For the TNM treatment, 1 mM cytochrome c in PBS was diluted with 10 mM sodium phosphate buffer (pH 8.0) to prepare 1 ml of $20\ \mu\text{M}$ cytochrome c. To this solution, $1.19\ \mu\text{l}$ of 10% (v/v) TNM solution in ethanol was added, and mixed vigorously for 1 h at room temperature. The reaction was terminated by gel filtration through Sephadex G-25 with PBS, and the concentration of cytochrome c was adjusted according to the absorbance at 409 nm.

In Vitro Caspase Activation Assay The caspase activa-

tion assay in a cell-free system was carried out using a cytosolic fraction of C6 cells and exogenous cytochrome c.^{26,27} Intact C6 cells were gently washed and harvested by scraping in PBS. The collected cells were washed with PBS again and precipitated at $200\ g$ for 5 min at room temperature. The cells were then resuspended in 3 times the volume of buffer A (250 mM sucrose, 20 mM Hepes-K [pH 7.5], 10 mM KCl, 1.5 mM MgCl_2 , 1 mM EDTA, 1 mM EGTA, 1 mM dithiothreitol) supplemented with $4\ \mu\text{g/ml}$ leupeptin, $2\ \mu\text{g/ml}$ pepstatin A, $2\ \mu\text{g/ml}$ aprotinin, 0.1 mM PMSF, and $25\ \mu\text{g/ml}$ *N*-acetyl-leucyl-leucyl-norleucine. The suspension was incubated on an ice bath for 15 min, and then the cells were homogenized with a glass homogenizer with 3 to 5 strokes of a pestle, or gently passed through a 22-gauge needle 15 times. The resulting cell homogenate was centrifuged at $7700\ g$ and the supernatants were subsequently centrifuged at $100000\ g$ for 30 min at 4°C . The supernatant was collected as a cytosolic fraction (S-cytosol). The S-cytosol fraction did not contain cytochrome c, as confirmed by immunoblotting with the anti-cytochrome c antibody (1:1000 dilution, mouse IgG clone 7H8.2C12, BD Biosciences, San Jose, CA, U.S.A.). The protein concentrations of the obtained S-cytosol fractions ranged from 2.5 to 5 mg protein/ml.

For *in vitro* caspase activation assay, the peroxynitrite-treated or control cytochrome c (800 nM) was added to the S-cytosol fraction (2.5 mg protein/ml) with or without addition of 0.5 mM ATP. The mixture was incubated at 30°C for 90 min, and the proteins were denatured by boiling for 10 min in a SDS sample buffer. The samples were subsequently subjected to SDS-PAGE (15% gel) and immunoblotting with the anti-cleaved caspase-3 antibody (1:1000 dilution, Cell Signaling Technology, Inc., Danvers, MA, U.S.A.) and visualized by chemiluminescence with ECL-plus reagents (Amersham Biosciences Corp., Piscataway, NJ, U.S.A.).

Detection of Nitrotyrosine in Hydrolysate of Peroxynitrite-Treated Cytochrome c Peroxynitrite-treated cytochrome c was hydrolyzed enzymatically as reported previously.²³ The hydrolysate of peroxynitrite-treated cytochrome c was centrifuged at $175\ g$ for 2 min, and the supernatant was analyzed by HPLC with a multi-wavelength detector (JASCO Co., Ltd., Tokyo, Japan) and an octadecylsilyl (ODS) column (TSK-GEL ODS-80Ts, $4.6\times 150\ \text{mm}$, Tosoh, Tokyo, Japan). As a mobile phase, 0.1 M potassium phosphate buffer (pH 3.5) containing 5% (v/v) methanol was used. The elution of tyrosine and nitrotyrosine was confirmed by comparison of the retention time with the authentic compounds.

HPLC and Mass Spectral Measurement of Tryptic Peptides from Nitrated Cytochrome c Peroxynitrite-treated cytochrome c ($20\ \mu\text{M}$) was concentrated with a centrifugal concentrator with a polyethylenesulfonate membrane and molecular weight cut-off at 5000. The concentrated cytochrome c was washed once by a centrifugal concentrator with an ammonium carbonate solution (0.1 M, pH 8.0), and adjusted to 1.28 mM with the washing solution. A proteomic grade of trypsin (Sigma, St. Louis, MO, U.S.A.) was reconstituted with 1 mM HCl according to the manufacturer's instruction and added to the cytochrome c solution at a ratio of 1:100 (w/w) as the amount of proteins. The mixture was incubated at 37°C for 16 h for tryptic digestion. The obtained tryptic peptides were analyzed with matrix-associated laser

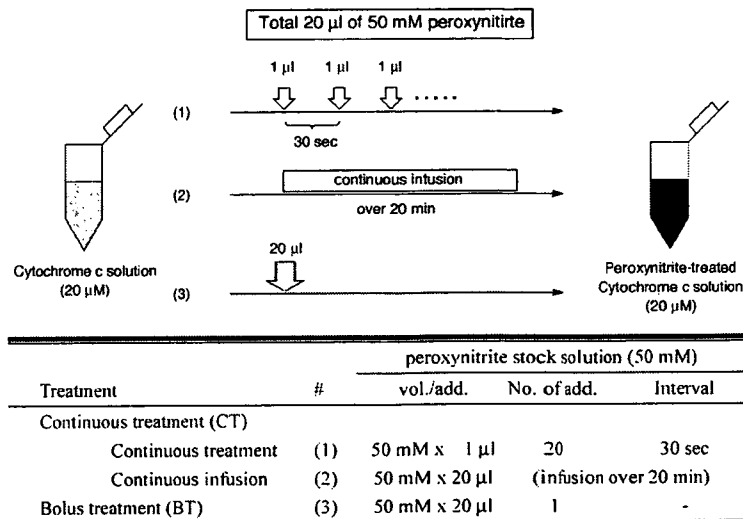


Chart 1. Preparation of Peroxynitrite-Treated Cytochrome c

dissorption ionization-time of flight mass spectrometry (MALDI-TOFMS), and the mass data were searched for peptide mass finger-printing databases to confirm the appropriate digestion of cytochrome c protein. Furthermore, the digested tryptic peptides were also subjected to a reversed-phase HPLC analysis with a linear gradient of 0 to 45% (v/v) acetonitrile in 0.1% (v/v) trifluoroacetic acid in 60 min, by monitoring with a multi-wavelength detector. The eluted peptide fractions were collected and lyophilized. Each fraction was reconstituted with H₂O/acetonitrile (8 : 2) and analyzed with MALDI-TOFMS. The digested peptide fragments were compared for the observed mass data for each fragment with the calculated mass numbers of the possible tryptic peptide fragments. The tyrosine-, nitrotyrosine-, and tryptophan-containing peptides were compared by the absorption spectra of the peptide fragments obtained from the HPLC analysis with a multi-wavelength detector.

RESULTS

Nitration of Cytochrome c by Continuous Peroxynitrite Infusion *in Vitro* We prepared peroxynitrite-treated cytochrome c in two different ways. One was a continuous infusion of peroxynitrite into cytochrome c in Earle's balanced salt solution (EBSS), and the other was a bolus treatment of cytochrome c with peroxynitrite. Cytochrome c treated with a continuous addition of peroxynitrite solution at 1-min intervals was also prepared. The cumulative final concentration of peroxynitrite was the same in all treatments. In all the preparations of peroxynitrite-treated cytochrome c, tyrosine nitration was confirmed by the detection of 3-nitrotyrosine in the pronase-digested hydrolysates of treated cytochrome c by an HPLC analysis of aromatic amino acid (Fig. 1).

To address the difference in the nitration sites between both nitrated cytochrome c preparations, the continuous and bolus peroxynitrite-treated cytochrome c were subjected to trypsin digestion, HPLC analysis, and MALDI-TOF mass spectrometry. The tryptic peptides of either continuous or bolus peroxynitrite-treated cytochrome c were first resolved by HPLC (Fig. 2). The chromatogram monitoring at 364 nm,

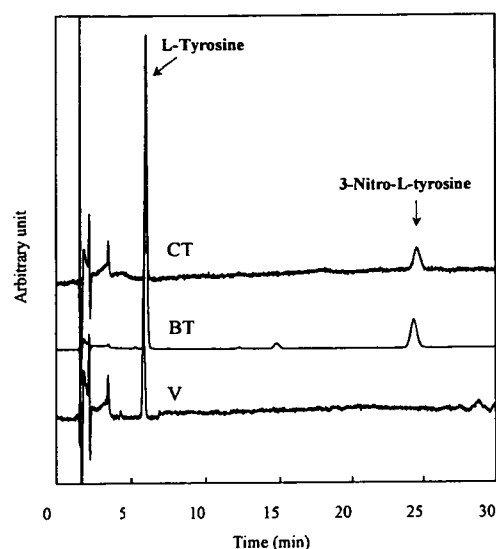


Fig. 1. Detection of Nitrotyrosine in Peroxynitrite-Treated Cytochrome c

Peroxynitrite-treated cytochrome c was hydrolyzed enzymatically, and subjected HPLC analysis for detection of nitrotyrosine. The labels CT, BT, and V on the chromatograms indicate the cytochrome c samples with the continuous, single-dose (bolus), and control (vehicle) treatment of peroxynitrite, respectively.

which is a local absorption maximum wavelength in nitrotyrosine, revealed that 4 peptide fragments contained nitrotyrosine residues in both groups treated with continuous and bolus treatment of peroxynitrite. The chromatogram at 215 nm revealed that the 3 peptide peaks (a, c, i) decreased with peroxynitrite treatment, concomitantly with the increase of the nitrated peptide peaks (b, d, g, j), without any changes in the other tryptic peptides in the chromatogram. Furthermore, from the spectra of these decreasing peaks, it was also confirmed that these peptides contained tyrosine residues. The fractionated tryptic peptides, including tyrosine- and nitrotyrosine-containing peptides, were subjected to a MALDI-TOF mass spectrometer and analyzed with both peptide mass fingerprinting from the public databases and the peptide molecular masses measured. From these results, it was revealed that at least 3 of the 4 tyrosine residues (Y48, Y67, Y74) in

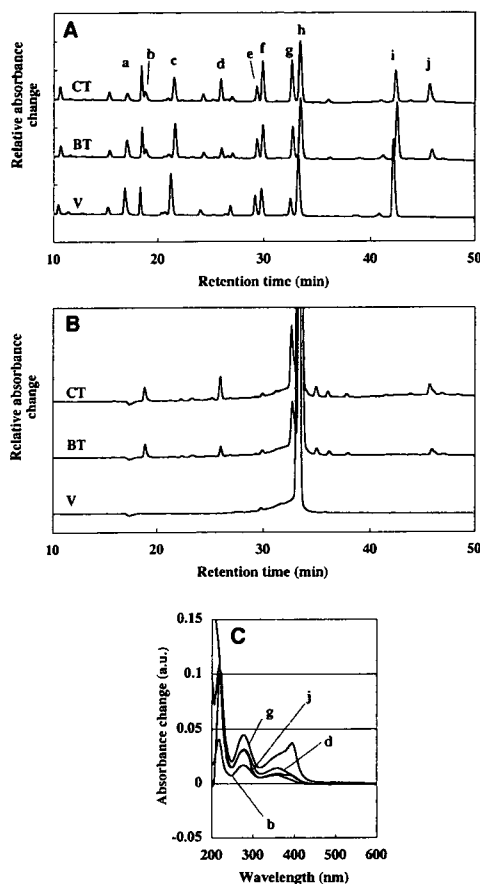


Fig. 2. Chromatogram and Absorption Spectra of the Tryptic Peptides of Peroxynitrite-Exposed Cytochrome c

Cytochrome c treated with peroxynitrite was dialyzed against ammonium carbonate, and digested with a sequencing grade of trypsin for 16 h at 37 °C. The resulting tryptic peptides were separated by HPLC with an ODS column and detected with a multi-wavelength absorption detector. A: chromatograms at 215 nm, B: chromatograms at 364 nm, C: absorption spectra of the nitrated peptide peaks. Small letter alphabetic labels on the peptide peaks and spectra correspond to the labels shown in Table 1. The labels CT, BT, and V on the chromatograms indicate the cytochrome c samples with the continuous, single-dose (bolus), and control (vehicle) treatment of peroxynitrite, respectively.

cytochrome c were nitrated without any detectable changes in the other peptide fragments under the conditions of the peroxynitrite treatment in this study (Fig. 2, Table 1). The peptide fragment containing tyrosine 74 (peak a in Fig. 2) was decreased by treatment of peroxynitrite, and the corresponding nitrated peptide (peak d in Fig. 2) was concomitantly increased. Although peak d also contained a certain amount of nitrated peptide containing tyrosine 48 (Table 1), it was found that the corresponding unnitrated fragment (peak c in Fig. 2) was only slightly decreased.

When we focused on the differences between the continuous and bolus peroxynitrite treatment, it was found that nitration at tyrosine 74 was specifically enhanced, and the nitration at tyrosine 67 was also slightly enhanced in cytochrome c with continuous treatment with peroxynitrite. The amount of nitrated cytochrome c (at any tyrosine residue) was 1.6 times larger by continuous treatment than by bolus treatment (Table 2). Whereas, nitration in tyrosine 74 is 4.2 times more frequent in continuously peroxynitrite-treated cytochrome c than in bolus peroxynitrite-treated (Table 3). There were no differences in the nitration at the other tyrosine residues (Fig.

Table 1. Assignment of Tryptic Peptides Based on the Observed Mass Numbers in Mass Spectrometry

Tryptic peptide	Mass number		Peak label ^{a)}
	Calculated	Observed	
Y ⁷⁴ IPGTK ⁷⁹	677.76	678.08	a
Y ⁷⁴ IPGTKMIFAGIK ⁸⁶ -NO ₂	1483.73	1485.25	d
T ²⁸ GPNLHGLFGR ³⁸	1168.27	1168.56	e or f ^{b)}
T ⁴⁰ GQAPGFSY ⁴⁸ TDANK ⁵³	1456.44	1456.09	c
T ⁴⁰ GQAPGFSY ⁴⁸ TDANK ⁵³ -NO ₂	1501.44	1501.44	d
E ⁹² DLIAI ⁹⁷ LKKATNE ¹⁰⁴	1507.63	1504.48	g ^{c)}
I ⁹ FVQKCAQCHTVEK ²²	1633.89	1633.61	h ^{c)}
G ⁵⁶ ITWGEETLMEY ⁶⁷ LENPK ⁷²	2010.17	2009.56	i
G ⁵⁶ ITWGEETLMEY ⁶⁷ LENPK ⁷² -NO ₂	2055.17	2054.06	j

a) The letter indicates the corresponding peak label in the chromatogram shown in Fig. 2. b) Peak e and f could not be separately fractionated for the mass measurement. c) Assignment of peak g and peak h are also based on their absorption spectra in addition to this peptide mass measurement. Peak h showed a unique absorption around 400 nm based on the heme, which attaches to two cysteine residues of Cys14 and Cys17.

Table 2. Relative Nitrotyrosine Content in Peroxynitrite-Treated Cytochrome c

Treatment	Nitrated cytochrome c (% ^{a)})	Fold increase ^{c)}
Continuous treatment (CT)	37.4 ± 0.37 ^{b)}	1.6
Bolus treatment (BT)	23.4 ± 0.27 ^{b)}	1
Vehicle (V)	0.70 ^{c)}	—

a) Percentage for cytochrome c with 3-nitrotyrosine: Since cytochrome c contains 4 tyrosine residues per molecule, the ratio (%) of nitrated cytochrome c were calculated by dividing the amount of 3-nitrotyrosine by 1/4 amount of total tyrosine. b) Mean ± S.D. from three independent experiments. c) Potency of a continuous treatment for nitration compared with that of a bolus treatment.

Table 3. Relative Nitration of Tyrosine 74 Containing Peptide

Treatment	Relative nitration ^{a)}
Continuous treatment (CT)	4.25 (4.22, 4.27) ^{b)}
Bolus treatment (BT)	1 (1.30, 0.70) ^{b)}
Vehicle (V)	0.03 (0.05, 0.01) ^{b)}

a) Relative amount of the nitrated peptide containing tyrosine 74 based on the amount of nitration by a bolus treatment. b) The value indicates the average of two independent experiments showing individual values in parentheses.

2, Table 1). When peroxynitrite was infused over more than 4 h, cytochrome c nitration was not observed.

In Vitro Apoptosis Assay with Peroxynitrite-Exposed Cytochrome c The ability of tyrosine-nitrated cytochrome c to cause caspase activation was evaluated by an *in vitro* apoptosis assay. Chemically modified cytochrome c was added to an intact cytosolic fraction from C6 cells and incubated at 30 °C for 90 min. For the detection of caspase activation, cleaved caspase-3 fragments (p17, p19) were observed *via* immunoblotting analysis with the specific antibody for the cleaved fragments of caspase-3. With the nitrated cytochrome c that had been continuously treated with peroxynitrite, caspase activation was not observed in the assay, while the activation was observed when the control and the intact cytochrome c preparations were used. With the TNM-treated cytochrome c, caspase activation was also attenuated (Figs. 2, 3). Interestingly, caspase activation was observed with the cytochrome c preparation treated with a bolus (1 mM) of peroxynitrite (Fig. 3). The activation was also observed with cytochrome c treated with a single low dose (50 μM) of perox-

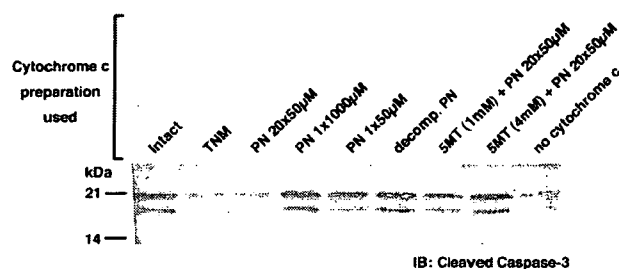


Fig. 3. Detection of Caspase-3 Fragments after *in Vitro* Caspase Activation Reaction with Exogenous Cytochrome c Nitrated by Continuous Peroxynitrite Treatment

Cytosolic fraction prepared from the intact cells was incubated with the cytochrome c preparations independently pretreated as indicated on the top of each lane. Caspase-3 active fragments (p17, p19) were observed with the specific antibody using chemiluminescence detection. TNM: tetranitromethane, PN: peroxynitrite, decomp. PN: decomposed PN, SMT: 5-methoxytryptamine. PN 20×50 µM indicates 20 times of continuous treatment with 50 µM peroxynitrite. Representative data of the same results from three independent experiments are shown.

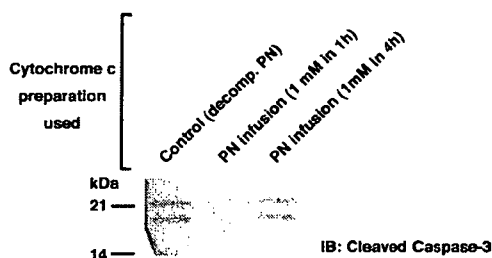


Fig. 4. Detection of Caspase-3 Fragments after the *in Vitro* Caspase Activation Reaction with the Exogenous Cytochrome c Nitrated by Continuous Peroxynitrite Exposure

Cytosolic fraction prepared from the intact cells was incubated with the cytochrome c preparations independently pretreated with peroxynitrite as indicated. The caspase-3 active fragments (p17, p19) were observed in the same way as in Fig. 3. PN: peroxynitrite, decomp. PN: decomposed PN, "PN 1 mM in 1 h" indicates that peroxynitrite was infused into the cytochrome c solution for 1 h, and the total cumulative concentration of peroxynitrite was 1 mM.

nitrite. From these results, it was found that the ability of cytochrome c to induce the caspase cascade activation was attenuated by continuous or repeated peroxynitrite exposure, but not by a bolus treatment. For further investigation regarding whether this functional loss with continuous treatment of peroxynitrite depends on the nitration of cytochrome c or not, a nitration-specific peroxynitrite scavenger, 5-methoxytryptamine (SMT), was employed. SMT has been found to inhibit tyrosine nitration by peroxynitrite without affecting the tyrosine-oxidizing activity.²⁸⁾ In the presence of SMT, cytochrome c was treated with peroxynitrite repeatedly, and this cytochrome c preparation was then subjected to an *in vitro* apoptosis assay. The result indicated that simultaneous SMT treatment preserved the ability of cytochrome c to induce caspase activation with continuous peroxynitrite exposure (Fig. 4). Together with the results from the *in vitro* apoptosis assay, it was found that continuous exposure of peroxynitrite caused the nitration of cytochrome c and the attenuation of its ability for caspase activation. However, a bolus of peroxynitrite exposure did not show this effect, even though the treated cytochrome c was nitrated.

DISCUSSION

From the *in vitro* apoptosis assay, it was found that caspase

cascade activation was suppressed when cytochrome c was treated with continuous peroxynitrite exposure, but this effect was not observed with a bolus treatment of peroxynitrite. We suggest that the attenuation of cytochrome c activity for caspase activation was closely related to tyrosine nitration because SMT, a nitration-specific scavenger, preserved the activity of cytochrome c (Fig. 3). Our results from a bolus treatment of cytochrome c with peroxynitrite is consistent with a previous report,²⁴⁾ in which cytochrome c treated with a bolus of peroxynitrite did not lose its ability for caspase cascade activation.

From the analysis of peroxynitrite-treated cytochrome c, it was found that all 4 positions of the tyrosine residues were nitrated in both methods of treatment. However, the tyrosine nitration at position 74 was increased when cytochrome c was exposed to continuous peroxynitrite treatment, compared with a bolus of peroxynitrite (Fig. 2, Table 1), although other tyrosine residues were nitrated to a similar extent with both treatments. By continuous treatment with peroxynitrite, the total amount of nitration to cytochrome c increased in some extent, but tyrosine 74 is more specifically nitrated by continuous treatment than by bolus treatment (Tables 2, 3). This suggests that continuous exposure of peroxynitrite is not only different from bolus one in the total amount of nitration, but also in the specificity of nitration. Based on the HPLC and MALDI-TOFMS analyses of the tryptic peptides of peroxynitrite-treated cytochrome c, methionine oxidation and modifications other than tyrosine nitration were not observed.

Our results suggest that the differential effect of continuous peroxynitrite exposure to cytochrome c on its potency for caspase activation depends on the extent of the nitration at tyrosine 74.

The tyrosine 74 residue is known to be important for the electron transfer reaction in mitochondria^{29,30)} and is located near the tyrosine 67 residue, which is the primary target for bolus peroxynitrite treatment.²²⁾ Cytochrome c exposed to a low dose of peroxynitrite impaired electron transfer ability, as shown in our previous study.²³⁾

From the spectral analysis of nitrated cytochrome c, there was almost no difference between the nitrated and control cytochrome c except a slight (less than 2 nm) shift of the Soret band. This band shift may reflect a slight change of the coordination conditions. Additionally, HPLC and MALDI-TOFMS analyses also suggest that there are no other detectable changes in the tryptic digest of the protein, except nitration of 3 tyrosine residues. Based on these observations, the differences between these 2 nitrated cytochrome c preparations can be attributed to the enhanced nitration of a specific tyrosine residue. These results implicate that the pattern of peroxynitrite exposure (continuous or bolus) results in different modifications at a specific tyrosine residue, and finally in different effects on caspase cascade activity. The redox status of cytochrome c is known to be involved in caspase activation. In this study, all the cytochrome c preparations, including the controls, were used in the oxidized form, as confirmed by the measurement of the absorption spectra of the samples. In this study, the mechanism of cytochrome c inactivation by peroxynitrite treatment was not fully revealed yet. It is known that cytochrome c interacts with apoptotic protease activating factor-1 (Apaf-1). It is possible that enhancement of Tyr 74 ni-

tration in cytochrome c may reduce its interaction with Apaf-1 or increase its dominant negative property. Although the molecular mechanisms of apoptosome inactivation by the specific nitration of cytochrome c still need to be clarified, our findings suggest that the nitration status at specific tyrosine residues can affect the ability of cytochrome c to cause caspase activation. It is known that cytochrome c interacts with Apaf-1 to form an active apoptosome complex. The enhanced nitration at tyrosine 74 may affect active apoptosome formation.

In conclusion, this study determined that cytochrome c nitrated by continuous treatment with peroxynitrite lost its ability to cause caspase cascade activation *in vitro*, whereas cytochrome c nitrated by a bolus peroxynitrite treatment had preserved activity. The differential property of the continuously peroxynitrite-exposed cytochrome c was closely related to the enhanced nitration of specific tyrosine residues. This is the first study to demonstrate that protein nitration at specific residues affects caspase activation. We suggest that the exposure pattern of peroxynitrite, including the duration and concentration, is important for cytochrome c activity for caspase activation.

Acknowledgments This work was supported in part by Grants-in-Aid for Scientific Research (No. 13771417 for H.N.) from the Ministry of Education, Culture, Sports, Science, and Technology, Japan.

REFERENCES

- Virag L., Szabo E., Gergely P., Szabo C., *Toxicol. Lett.*, **140–141**, 113–124 (2003).
- Ferdinandy P., Schulz R., *Br. J. Pharmacol.*, **138**, 532–543 (2003).
- Ronson R. S., Nakamura M., Vinten-Johansen J., *Cardiovasc. Res.*, **44**, 47–59 (1999).
- White B. C., Sullivan J. M., DeGracia D. J., O'Neil B. J., Neumar R. W., Grossman L. I., Rafols J. A., Krause G. S., *J. Neurol. Sci.*, **179**, (S 1–2), 1–33 (2000).
- Ste-Marie L., Hazell A. S., Bemeur C., Butterworth R., Montgomery J., *Brain Res.*, **918**, 10–19 (2001).
- Gursoy-Ozdemir Y., Bolay H., Sariibas O., Dalkara T., *Stroke*, **31**, 1974–1980, discussion 1981 (2000).
- Eliasson M. J., Huang Z., Ferrante R. J., Sasamata M., Molliver M. E., Snyder S. H., Moskowitz M. A., *J. Neurosci.*, **19**, 5910–5918 (1999).
- Giasson B. I., Duda J. E., Murray I. V., Chen Q., Souza J. M., Hurtig H. I., Ischiropoulos H., Trojanowski J. Q., Lee V. M., *Science*, **290**, 985–989 (2000).
- Good P. F., Hsu A., Werner P., Perl D. P., Olanow C. W., *J. Neuropathol. Exp. Neurol.*, **57**, 338–342 (1998).
- Pennathur S., Jackson-Lewis V., Przedborski S., Heinecke J. W., *J. Biol. Chem.*, **274**, 34621–34628 (1999).
- Castegna A., Thongboonkerd V., Klein J. B., Lynn B., Markesbery W. R., Butterfield D. A., *J. Neurochem.*, **85**, 1394–1401 (2003).
- Luth H. J., Munch G., Arendt T., *Brain Res.*, **953**, 135–143 (2002).
- Hensley K., Maidt M. L., Yu Z., Sang H., Markesbery W. R., Floyd R. A., *J. Neurosci.*, **18**, 8126–8132 (1998).
- Smith M. A., Richey Harris P. L., Sayre L. M., Beckman J. S., Perry G., *J. Neurosci.*, **17**, 2653–2657 (1997).
- Beal M. F., Ferrante R. J., Browne S. E., Matthews R. T., Kowall N. W., Brown R. H., Jr., *Ann. Neurol.*, **42**, 644–654 (1997).
- Abe K., Pan L. H., Watanabe M., Kato T., Itoyama Y., *Neurosci. Lett.*, **199**, 152–154 (1995).
- Duda J. E., Giasson B. I., Chen Q., Gur T. L., Hurtig H. I., Stern M. B., Gollomp S. M., Ischiropoulos H., Lee V. M., Trojanowski J. Q., *Am. J. Pathol.*, **157**, 1439–1445 (2000).
- Aoyama K., Matsubara K., Fujikawa Y., Nagahiro Y., Shimizu K., Umegae N., Hayase N., Shiono H., Kobayashi S., *Ann. Neurol.*, **47**, 524–527 (2000).
- Lanone S., Manivet P., Callebort J., Launay J. M., Payen D., Aubier M., Boczkowski J., Mebazaa A., *Biochem. J.*, **366**, 399–404 (2002).
- Kooy N. W., Lewis S. J., Royall J. A., Ye Y. Z., Kelly D. R., Beckman J. S., *Crit. Care Med.*, **25**, 812–819 (1997).
- Sampson J. B., Ye Y., Rosen H., Beckman J. S., *Arch. Biochem. Biophys.*, **356**, 207–213 (1998).
- Cassina A. M., Hodara R., Souza J. M., Thomson L., Castro L., Ischiropoulos H., Freeman B. A., Radi R., *J. Biol. Chem.*, **275**, 21409–21415 (2000).
- Nakagawa H., Ohshima Y., Takusagawa M., Ikota N., Takahashi Y., Shimizu S., Ozawa T., *Chem. Pharm. Bull.*, **49**, 1547–1554 (2001).
- Ueta E., Kamatani T., Yamamoto T., Osaki T., *Int. J. Cancer*, **103**, 717–722 (2003).
- Pryor W. A., Cueto R., Jin X., Koppenol W. H., Ngu-Schwemlein M., Squadrito G. L., Uppu P. L., Uppu R. M., *Free Radic Biol. Med.*, **18**, 75–83 (1995).
- Liu X., Kim C. N., Yang J., Jemmerson R., Wang X., *Cell*, **86**, 147–157 (1996).
- Hampton M. B., Zhivotovsky B., Slater A. F., Burgess D. H., Orrenius S., *Biochem. J.*, **329**, 95–99 (1998).
- Nakagawa H., Sumiki E., Ikota N., Matsushima Y., Ozawa T., *Antioxid. Redox. Signal*, **1**, 239–244 (1999).
- Takano T., Kallai O. B., Swanson R., Dickerson R. E., *J. Biol. Chem.*, **248**, 5234–5255 (1973).
- Takano T., Trus B. L., Mandel N., Mandel G., Kallai O. B., Swanson R., Dickerson R. E., *J. Biol. Chem.*, **252**, 776–785 (1977).

ORIGINAL ARTICLE

Proteome analyses of the growth inhibitory effects of NCH-51, a novel histone deacetylase inhibitor, on lymphoid malignant cells

T Sanda^{1,2}, T Okamoto¹, Y Uchida¹, H Nakagawa³, S Iida², S Kayukawa², T Suzuki³, T Oshizawa⁴, T Suzuki⁴, N Miyata³ and R Ueda²

¹Department of Molecular and Cellular Biology, Nagoya City University Graduate School of Medical Sciences, Nagoya, Japan; ²Department of Internal Medicine and Molecular Science, Nagoya City University Graduate School of Medical Sciences, Nagoya, Japan; ³Department of Organic and Medicinal Chemistry, Nagoya City University Graduate School of Pharmaceutical Sciences, Nagoya, Japan and ⁴Department of Cellular and Gene Therapy Products, National Institute of Health Sciences, Tokyo, Japan

Recent reports showing successful inhibition of cancer and leukemia cell growth using histone deacetylase inhibitor (HDACi) compounds have highlighted the potential use of HDACi as anti-cancer agents. However, high incidence of toxicity and low stability *in vivo* were observed with hydroxamic acid-based HDACi such as suberoylanilide hydroxamic acid (SAHA), thus limiting its clinical applicability. In this study, we found that a novel non-hydroxamate HDACi NCH-51 could inhibit the cell growth of a variety of lymphoid malignant cells through apoptosis induction, more effectively than SAHA. Activation of caspase-3, -8 and -9, but not -7 was detected after the treatment with NCH-51. Gene expression profiles showed that NCH-51 and SAHA similarly upregulated *p21* and down-regulated anti-apoptotic molecules including *survivin*, *bcl-w* and *c-FLIP*. Proteome analysis using two-dimensional electrophoresis revealed that NCH-51 upregulated anti-oxidant molecules including peroxiredoxin 1 and 2 and glutathione S-transferase at the protein level. Interestingly, NCH-51 induced reactive oxygen species (ROS) after 8h whereas SAHA continuously declined ROS. Pretreatment with an antioxidant, N-acetyl-L-cysteine, abolished the cytotoxicity of NCH-51. These findings suggest that NCH-51 exhibits cytotoxicity by sustaining ROS at the higher level greater than SAHA. This study indicates the therapeutic efficacy of NCH-51 and novel insights for anti-HDAC therapy.

Leukemia advance online publication, 9 August 2007;
doi:10.1038/sj.leu.2404902

Keywords: histone deacetylase; apoptosis; reactive oxygen species; peroxiredoxin

Introduction

Histone deacetylase (HDAC) is responsible for deacetylation of histone or non-histone substrates.^{1–3} Deacetylation of histone converts local chromatin into repressive configuration, resulting in the transcriptional repression.^{2,3} The aberrant recruitment of HDAC is closely associated with leukemogenesis through silencing of expression of the genes involved in hematopoietic cell differentiation.⁴ In addition, subsequent studies demonstrated that the malignant phenotypes of solid tumors could be ascribed to the aberrant activation of HDAC and deacetylation of the histone proteins adjacent to tumor suppressor genes.^{5,6} Thus, a number of small-molecule HDAC

inhibitors (HDACi) have been developed as anti-cancer agents.^{1,7} In fact, HDACi compounds were shown to induce cell cycle arrest, differentiation and apoptosis in a variety of malignant cells.^{1,7}

Suberoylanilide hydroxamic acid (SAHA) (also known as vorinostat) belongs to a hydroxamic acid-based hybrid polar compound and is a prototypic compound of HDACi.⁷ Phase I clinical trials with refractory solid tumors and hematological malignancies by SAHA revealed frequent toxicities including dehydration, fatigue, diarrhea, anorexia and cytopenia, in spite of significant clinical benefits.⁸ In addition, a poor pharmacokinetics of SAHA was noted.⁸ Other hydroxamic acid-based derivatives showed similar therapeutic profiles.^{9,10} Thus, we have attempted to develop a non-hydroxamate HDACi to overcome these problems. A novel HDACi NCH-51 was designed based on SAHA by replacement of the hydroxamic acid by acylated thiol group. NCH-51 could inhibit HDACs as strongly as SAHA and inhibited the cell growth of various solid tumor cell lines *in vitro* (mean IC₅₀ values of NCH-51 and SAHA are 3.8 and 3.7 μM, respectively).¹¹ Unlike SAHA, NCH-51 is stable in human plasma at the remaining rate of approximately 51% after 24 h of administration (unpublished data).

Recent findings suggest that HDACi may have additional effects other than transcriptional interference. Although it is well established that HDACi upregulates gene expression of tumor suppressors such as *p21* through histone hyperacetylation,^{12–14} HDACi does not always upregulate gene expression but induces malignant cell death by downregulating gene expression such as anti-apoptotic genes. In addition, some HDACi compounds exhibited anti-cancer effects through acetylation of non-histone substrates such as heat-shock protein 90 (HSP90),¹⁵ α-tubulin,¹⁶ p53¹⁷ and nuclear factor-κB.¹⁸ For example, Bali *et al.*¹⁵ reported that HDACi caused leukemia cell death by hyperacetylation of HSP90. Hideshima *et al.*¹⁹ demonstrated that tubacin, a specific HDAC6 inhibitor, was effective in augmenting cell death mediated by bortezomib, a proteasome inhibitor, by inhibiting the protein degradation through blocking aggresome activity. Thus, the cell growth inhibitory action of HDACi could be exhibited at the protein expression level.

Here we demonstrate the therapeutic efficacy of NCH-51 on lymphoid malignant cells. NCH-51 induced cell death, more strongly than SAHA. We analyzed the protein expression profiles and found that NCH-51 modulated the expression of antioxidant molecules at the protein level. NCH-51 sustained the intracellular reactive oxygen species (ROS) greater than SAHA.

Correspondence: Professor T Okamoto, Department of Molecular and Cellular Biology, Nagoya City University Graduate School of Medical Sciences, 1 Kawasumi, Mizuho-cho, Mizuho-ku, Nagoya, Aichi 467-8601, Japan.

E-mail: tokamoto@med.nagoya-cu.ac.jp

Received 22 March 2007; revised 6 June 2007; accepted 11 July 2007